

1 Mechanistic Insights of High Temperature-Interfered 2 Meiosis in Autotetraploid *Arabidopsis thaliana*

3
4 Huiqi Fu¹, Ke Yang¹, Xiaohong Zhang^{1,2}, Jiayi Zhao¹, Ibrahim Eid Elesawi^{3,4}, Hong Liu²,
5 Jing Xia², Guanghui Yu², Chunli Chen^{3,5}, Chong Wang⁶, Bing Liu^{1*}

6 ¹8A-506, Laboratory of Plant Meiosis and Reproduction, College of Life Sciences,
7 South-Central University for Nationalities, Wuhan 430074, China;

8 ²College of Life Sciences, South-Central University for Nationalities, Wuhan 430074, China;

9 ³College of Life Science and Technology, Huazhong Agricultural University, Wuhan, 430070;

10 ⁴Agricultural Biochemistry Department, Faculty of Agriculture, Zagazig University, Zagazig
11 44511, Egypt;

12 ⁵Key Laboratory of Plant Resource Conservation and Germplasm Innovation in Mountainous
13 Region (Ministry of Education), Institute of Agro-bioengineering, College of Life Science,
14 Guizhou University, Guiyang 550025, China;

15 ⁶College of Life Sciences, Shanghai Normal University, Shanghai 200234, China;

16 *To whom correspondence should be addressed: Bing Liu (bl472@scuec.edu.cn).

17

18 Abstract

19

20 Environmental temperature has a huge impact on multiple meiosis processes in flowering
21 plants. Polyploid plants derived from whole genome duplication are believed to have an
22 enhanced abiotic stress tolerance. In this study, the impact of high temperatures on male
23 meiosis in autotetraploid *Arabidopsis thaliana* was investigated. We found that autotetraploid
24 Columbia (Col-0) plants generate a subpopulation of aberrant meiotic products under normal
25 temperature, which is significantly increased under heat stress. Cytological studies revealed
26 that, as the case in diploid *Arabidopsis thaliana*, assembly of microtubular cytoskeleton
27 network, pairing and segregation of homologous chromosomes, and meiotic recombination in
28 autotetraploid *Arabidopsis* are compromised under the high temperatures. Immunostaining of
29 γ H2A.X and recombinase DMC1 suggested that heat stress inhibits formation of DNA
30 double-strand breaks; additionally, it specifically destabilizes ASY1 and ASY4, but not SYN1
31 on chromosomes. The loading defects of ASY1 and ASY4 overlap in the *syn1* mutant, which
32 supports that the building of lateral element of synaptonemal complex occurs downstream of
33 a SYN1-ASY4-ASY3 stepwise assembly of axis. Remarkably, heat-induced abnormalities of
34 ASY1 and ASY4 co-localize on chromosomes of both diploid and autotetraploid *Arabidopsis*,
35 suggesting that high temperatures interfere with ASY1-associated SC via an impacted
36 stability of chromosome axis. Furthermore, ZYP1-dependent transverse filament of SC is
37 disrupted by heat stress. Taken together, these findings suggest that polyploidization
38 negatively contributes to instability of chromosome axis and meiotic recombination in
39 *Arabidopsis thaliana* under heat stress.

40

41 **Keywords**

42

43 Heat stress; chromosome segregation; meiotic recombination; DSB; chromosome axis;
44 synapsis; autotetraploid

45

46 **Introduction**

47

48 Meiosis is a specialized type of cell division that, in plants, occurs in pollen mother cells
49 (PMCs) and/or megasporocytes giving rise to gametes with halved ploidy. At early stages of
50 meiosis, meiotic recombination (MR) takes place between homologous chromosomes to drive
51 exchange of genetic information via formation of crossovers (COs). MR results in novel
52 combination of genetic alleles among progenies, which enables natural selection can happen
53 in the population, and safeguards balanced segregation of homologous chromosomes that is
54 vital for production of viable gametes and fertility (Wang and Copenhaver, 2018). MR is
55 initiated by the generation of DNA double-strand breaks (DSBs), which are catalyzed by
56 SPO11, a type-II topoisomerase (topoisomerase VI, subunit A) conserved among eukaryotes
57 (Bergerat et al., 1997; Da Ines et al., 2020; Grelon et al., 2001; Stacey et al., 2006). In
58 Arabidopsis, SPO11-1 and SPO11-2 are required for MR, while SPO11-3 plays a role in
59 endoreduplication (Grelon et al., 2001; Hartung et al., 2007; Stacey et al., 2006;
60 Sugimoto-Shirasu et al., 2002; Yin et al., 2002). Plants with defective DSB formation exhibit
61 impaired homolog synapsis and recombination, and are male sterile due to mis-segregation of
62 chromosomes (Da Ines et al., 2020; De Muyt et al., 2007; Grelon et al., 2001; Stacey et al.,
63 2006; Xue et al., 2018). DSBs are subsequently processed by recombinases RAD51, which
64 repairs DSBs using sister chromatids as a template that leads to non-crossovers (NCOs); or
65 DMC1, which drives MR-specific DSB repair (Da Ines et al., 2013; Klimyuk and Jones, 1997;
66 Kobayashi et al., 2019; Li et al., 2004; Pohl and Nickoloff, 2008; Sanchez-Moran et al., 2007;
67 Singh et al., 2017; Su et al., 2017; Yao et al., 2020). RAD51 and DMC1 do not act
68 independently, with RAD51 functioning as an accessory factor of DMC1 in catalyzing MR
69 (Cloud et al., 2012; Da Ines et al., 2013; Kurzbauer et al., 2012; Lan et al., 2020). There are
70 two types of COs, most of which (~85%) belong to type-I class catalyzed by ZMM proteins,
71 and are spaced on chromatin by interference (Higgins et al., 2004); while the other COs
72 (type-II) mediated by MUS81 are interference-insensitive (Berchowitz et al., 2007;
73 Hollingsworth and Brill, 2004).

74

75 DSB formation and MR rely on a programmed building of chromosome axis. Meiotic-specific
76 cohesion protein AtREC8/SYN1 binds sister chromatids together and aids the chromosomes
77 to form a loop structure (Shahid, 2020; Zickler and Kleckner, 1999). It is proposed that DSBs
78 are formed at the basal region of the loops that are anchored to the ASY1-associated lateral
79 element of synaptonemal complex (SC) (Kim and Choi, 2019; Zickler and Kleckner, 1999).
80 The coiled-coil axis proteins ASY3 and ASY4 play a key role in organizing axis formation,
81 and mediates the connections between the SYN1-mediated chromosome axis and SC via the
82 interplay with ASY1 (Chambon et al., 2018; Ferdous et al., 2012; Osman et al., 2018).

83 Dysfunction of the axis components causes disrupted axis structure and reduced DSB
84 formation, and consequently results in failed homolog synapsis and MR (Bai et al., 1999; Cai
85 et al., 2003; Chambon et al., 2018; Ferdous et al., 2012; Lambing et al., 2020b). SC formation
86 is essentially required for normal homolog synapsis and CO formation. ASY1 contributes to
87 CO formation via the DMC1-mediated MR pathway (Armstrong et al., 2002; Sanchez-Moran
88 et al., 2007). Meanwhile, ASY1 prevents the preferential occurrence of COs at distal regions
89 by antagonizing telomere-led recombination, and by maintaining CO interference along the
90 chromosomes (Lambing et al., 2020a). ZYP1 is a conserved transverse filament protein of SC
91 which is required for homolog synapsis (Barakate et al., 2014; Higgins et al., 2005; Wang et
92 al., 2010). Recent findings revealed that ZYP1-dependent SC formation is indispensable for
93 maintenance of interference, by which ZYP1 restricts the number of type-I COs along the
94 chromosomes; moreover, the bias of CO rate between sexes is wiped when ZYP1 is knocked
95 out (Capilla-Pérez et al., 2021; France et al., 2021). Homologous chromosomes are separated
96 by the bipolar pulling of spindles at the end of meiosis I (MI); and after meiosis II (MII),
97 sister chromatids disjoin with each other, which leads to production of four isolated
98 chromosome sets (Bhatt et al., 2001; Zamariola et al., 2014). In Arabidopsis, like other dicot
99 plants, meiotic cytokinesis takes place thereafter the completion of two rounds of
100 chromosome separation (De Storme and Geelen, 2013).

101

102 Male meiosis in plants is sensitive to variations of environmental temperature (Bomblies et al.,
103 2015; De Storme and Geelen, 2014; Liu et al., 2019; Lohani et al., 2019). In both dicots and
104 monocots, low temperatures predominantly affect cytokinesis by disturbing the formation of
105 phragmoplast, which thereby induces meiotic restitution and formation of unreduced gametes
106 (De Storme et al., 2012; Liu et al., 2018; Tang et al., 2011). In contrast, under high
107 temperatures, both chromosome dynamics and cytokinesis are prone to be impacted;
108 especially, the response of MR to heat stress is more complex (De Storme and Geelen, 2020;
109 Draeger and Moore, 2017; Lei et al., 2020; Mai et al., 2019; Ning et al., 2021; Wang et al.,
110 2017). In Arabidopsis, a mild increase of temperature (28°C) positively affects type-I CO rate
111 by enhancing the activity of ZMM proteins without impacting DSB formation (Lloyd et al.,
112 2018; Modliszewski et al., 2018). Under a higher temperature (32°C), however, the rate and
113 distribution of COs are altered (De Storme and Geelen, 2020). Moreover, at extreme high
114 temperatures (36-38°C) over the fertile threshold of Arabidopsis, occurrence of COs is fully
115 suppressed due to inhibited DSBs generation and impaired homolog synapsis; additionally,
116 the microtubular cytoskeleton-based chromosome segregation is disrupted (Lei et al., 2020;
117 Ning et al., 2021). Environmental temperatures therefore may manipulate genomic diversity,
118 and/or influence ploidy consistency of plants over generations by impacting male meiosis
119 during microsporogenesis (Bomblies et al., 2015; Lohani et al., 2019).

120

121 Most higher plants, especially for angiosperms, have experienced at least one episode of
122 whole genome duplication (WGD) event, which is considered an important force driving
123 speciation, diversification, and domestication (Del Pozo and Ramirez-Parra, 2015;
124 Dubcovsky and Dvorak, 2007; Leitch and Leitch, 2008; Ren et al., 2018; Soltis et al., 2015).
125 Polyploids are classified into autopolyploids and allopolyploids, which originate from
126 intraspecies WGD events, or arise from multiple evolutionary lineages through the

127 combination of differentiated genomes, respectively (Bretagnolle and Thompson, 1995;
128 Jackson and Chen, 2010; Parisod et al., 2010; Ramsey and Schemske, 1998; Soltis and Soltis,
129 2009). In autotetraploid plants, four intraspecies-homologues usually undergo randomly
130 separation at anaphase I; this is different as allotetraploids, in which subgenomes tend to
131 segregate independently due to CO formation between the genetically-closer pairs of
132 homologues (Ramsey and Schemske, 2002; Stift et al., 2008). It is believed that the increased
133 sets of homologous chromosomes contribute to genome flexibility and confer the plants with
134 enhanced tolerance to both endogenous genetic mutations, or exogenous environmental
135 stresses (Comai, 2005; Del Pozo and Ramirez-Parra, 2015; Rao et al., 2020; te Beest et al.,
136 2012; Van de Peer et al., 2020; Wu et al., 2020). However, the multiple chromosome sets also
137 challenge genome stability by impacting homolog pairing and balanced chromosome
138 segregation with associated reduced fertility or viability of plants (Comai, 2005; Otto, 2007;
139 Santos et al., 2003; Svačina et al., 2020; Yant et al., 2013). It is proposed that polyploids have
140 evolutionarily developed a moderate strategy that assures genome stability to a large scale by
141 early-stage homoeologous chromosome sorting, chromosome axis-mediated MR modification,
142 and/or by sacrificing an acceptable reduction of CO formation (Bomblies et al., 2016;
143 Grandont et al., 2014; Lloyd and Bomblies, 2016; Morgan et al., 2020; Seear et al., 2020).
144 However, it remains not yet clear how male meiosis in polyploid plants responds to increased
145 environmental temperatures.

146
147 In this study, we found that autotetraploid Col-0 plants incubated at 20°C produce a low but
148 consistently-detectable rate of abnormal meiotic products, suggesting that meiotic defects
149 naturally take place in autotetraploid *Arabidopsis*. We also showed that both the chromosome
150 dynamics and axis formation in the autotetraploid *Arabidopsis* plants are more sensitive to
151 high temperatures than that in diploid *Arabidopsis*, suggesting that a duplicated genome does
152 not confer a higher tolerance but instead increases chromosome instability in *Arabidopsis*
153 *thaliana* under thermal conditions. Remarkably, we provided evidence supporting that
154 ASY1-associated lateral element of SC formation relies on a SYN1-ASY4-ASY3 stepwise
155 assembly of chromosome axis, in which the stability of ASY4- and ASY3-mediated axis
156 bridges the impact of high temperature on SC organization. Overall, these findings provide
157 insights into how high temperatures affect male meiosis in autotetraploid *Arabidopsis*
158 *thaliana*.

159

160 **Results**

161

162 **Heat stress increases meiotic defects in autotetraploid *Arabidopsis thaliana***

163

164 To reveal the impact of heat stress on male meiosis of autotetraploid *Arabidopsis thaliana*, we
165 analyzed tetrad-staged PMCs in heat-stressed autotetraploid Col-0 plants by performing
166 orcein staining (Fig. 1). First, fluorescence in situ hybridization (FISH) using a
167 centromere-specific probe was applied in the autotetraploid Col-0 plants, which showed that
168 somatic cells harbored twenty chromosomes representing that the plants were tetraploid
169 (Supplement Fig. S1). In plants under control temperature, most PMCs (~95.46%) produced

170 tetrads that subsequently developed into normal-sized microspores with a single nucleus (Fig.
171 1A; B and E). Interestingly, a low proportion of polyads and/or unbalanced-tetrads was
172 consistently observed, which resulted in formation of microspores with varied sizes (Fig. 1A;
173 C, polyad, 3.67%; D, unbalanced-tetrad, 0.86%; F, microspores). These phenotypes suggested
174 that a minor frequency of meiotic defects naturally take place in autotetraploid *Arabidopsis*
175 *thaliana*. In plants stressed by 37°C, a significantly increased frequency (~92.49%) of
176 abnormal meiotic products was observed, in which unbalanced-triads, polyads and
177 unbalanced-tetrads occupied the highest proportions (Fig. 1A; M-O, unbalanced-triads,
178 29.02%; R and S, polyads, 26.42%; P and Q, unbalanced-tetrads, 26.17%). These figures,
179 together with the observed unbalanced-dyads that contained differently-numbered and/or
180 -sized nuclei (Fig. 1A, G, I and J, 7.25%), indicated that chromosome segregation in MI
181 and/or II was interfered. Meanwhile, the occurrence of balanced-dyad and balanced-triad
182 represented an induction of meiotic restitution (Fig. 1A; H, balanced-dyad, 2.85%; K,
183 balanced-triad, 0.78%). The defective tetrad stage PMCs led to generation of aneuploid
184 microspores at unicellular stage (Fig. 1T and U). Similar cellular alterations were observed in
185 autotetraploid Col-0 plants stressed by 32°C (Fig. 1A; V-Z). Moreover, we found that under
186 high temperatures, the flower buds with the same size as that in control occurring meiosis
187 and/or cytokinesis contained unicellular stage microspores, which hinted that the high
188 temperatures accelerated meiosis progressing (Supplement Fig. S2A-C).

189
190 We next stained meiotic cell walls using aniline blue to examine the impact of high
191 temperatures on meiotic cytokinesis in autotetraploid Col-0 plants. In line with the analysis by
192 orcein staining, most tetrads in control plants showed a regular ‘cross’-like cell wall
193 formation (Fig. 2A). Observation of polyad supported that meiotic defects naturally occurred
194 in the autotetraploid *Arabidopsis* (Fig. 2B). After incubation under 37°C, the autotetraploid
195 Col-0 plants showed defective meiotic cell wall formation including unbalanced-triads (Fig.
196 2C; Supplement Fig. S3F-I), polyad (Fig. 2D; Supplement Fig. S3K and L),
197 unbalanced-tetrads (Fig. 2E; Supplement Fig. S3E and J), unbalanced-dyad (Fig. 2F;
198 Supplement Fig. S3B-D), balanced-dyad (Fig. 2G; Supplement Fig. S3A) and balanced-triad
199 (Fig. 2H; Supplement Fig. S3E). These data demonstrated that heat stress interferes with one
200 or more meiosis processes; e.g. chromosome segregation and cytokinesis in autotetraploid
201 *Arabidopsis thaliana*.

202 203 **Microtubular cytoskeleton in autotetraploid *Arabidopsis* is abnormally assembled under** 204 **heat stress**

205
206 To address the cellular mechanism underlining heat-induced aberrant tetrad formation and
207 defective cytokinesis in autotetraploid *Arabidopsis*, we examined microtubular cytoskeleton
208 by performing immunostaining of α -tubulin (Fig. 3). In autotetraploid Col-0 plants incubated
209 at 20°C, formation of spindle was initiated at early metaphase I (Fig. 3A), and thereafter at
210 middle metaphase I, homologous chromosomes aligned at the cell plate when microtubule
211 arrays got attachment with the centromeres labeled by an anti-CENH3 antibody (Fig. 3B).
212 The monopolar pulling force from the spindle separated the homologous chromosomes at the

213 end of MI, and two spindles were formed at metaphase II to separate the sister chromatids
214 (Fig. 3C). At telophase II, mini-phragmoplast structures composed of radial microtubule
215 arrays (RMAs) were constructed between the four isolated nuclei (Fig. 3D). Notably, triad-
216 and poly-like configurations together with the occurrence of mini-nucleus (Fig. 3E and F)
217 supported existence of meiotic defects in control autotetraploid *Arabidopsis* plants. After heat
218 treatment, we found that the metaphase I microtubule arrays did not display a typical spindle
219 configuration, which bond with randomly-distributed univalent chromosomes (Fig. 3G and H).
220 The univalents and the impaired spindle led to unbalanced segregation of homologous
221 chromosomes at interkinesis, which, meanwhile, showed irregular and sparse phragmoplast
222 formation (Fig. 3I). Disrupted spindles were also observed at metaphase II (Fig. 3J). These
223 alterations resulted in generation of unbalanced-tetrad and polyad with omitted and/or
224 abnormally-shaped RMAs between the adjacent and/or differently-sized nuclei (Fig. 3K and
225 L).

226

227 **Heat stress interferes with chromosome behaviors in autotetraploid *Arabidopsis thaliana***

228

229 Chromosome behaviors in meiocytes of autotetraploid Col-0 plants were analyzed using
230 4',6-diamidino-2-phenylindole (DAPI) staining. In control plants, homologous chromosomes
231 synapsed at pachytene (Fig. 4A). However, unpaired chromosomes were occasionally
232 observed indicating a pairing defect (Fig. 4B). Bridge- and thick rope-like structures implied
233 irregular chromosome interactions (Fig. 4C and D, yellow and green arrows). At diakinesis
234 and metaphase I, most meiocytes showed existence of five tetravalents (Fig. 5E-G and I;
235 60.71%, n = 34). About 33.93% meiocytes showed a combination of bivalents and
236 tetravalents including PMCs containing four (21.43%, n = 12), three (8.93%, n = 5) and two
237 tetravalents (3.57%, n = 2) (Fig. 4H, J and K, red arrow). Additionally, we observed
238 meiocytes that harbored ten bivalents (Fig. 3L; 5.36%, n = 3). These suggested that synapsis
239 took place between four homologues or a couple of them, or occurred only between two
240 homologous chromosomes. Meanwhile, irregular connections hinted associations between
241 nonhomologous chromosomes (Fig. 4F, G and J, yellow arrows). After MI, most meiocytes
242 underwent balanced segregation of the four chromosome sets (Supplement Fig. S4A and D;
243 75%, n = 48), which resulted in generation of tetrads with four isolated nuclei each harboring
244 a halved chromosome number (Supplement Fig. S4G; 88.24%, n = 105). Unbalanced
245 separation of homologues with lagged chromosomes (Supplement Fig. S4B and C, E and F;
246 25%, n = 16) consequently led to defective tetrads (Supplement Fig. S4H-J; 11.76%, n =
247 14).

248

249 In autotetraploid Col-0 plants treated by 37°C, we observed bridge-like chromosome
250 structures at zygotene (Fig. 4M and N, yellow arrows); meanwhile, incomplete and/or
251 impaired pairing and synapsis were found on the pachytene chromosomes (Fig. 4O and P,
252 green arrows). These figures suggested that the high temperature induced abnormal
253 chromosome interactions and interfered with homolog synapsis. At diakinesis and metaphase
254 I, ~93.68% meiocytes showed twenty individual chromatids (Fig. 4Q-T, red arrow; n = 89),
255 which represented an omitted and/or suppressed CO formation that consequently resulted in
256 unbalanced chromosome segregation at anaphase I (98.08%, n = 51) and tetrad stage (97.67%,

257 n = 126) (Supplement Fig. S4K-T). Similarly, in autotetraploid Col-0 plants stressed under
258 32°C, failed and/or irregular chromosome pairing and synapsis were induced (Fig. 4U and V,
259 green arrows); in the meantime, a combination of univalents, bivalents and multivalents
260 suggested that CO formation was compromised (Fig. 4W and X, red arrows) which led to
261 unbalanced chromosome segregation at MII (Supplement Fig. S4U-Y). Taken together, these
262 findings revealed that heat stress interferes with chromosome pairing and/or synapsis, and
263 segregation in autotetraploid Arabidopsis.

264

265 **High temperatures reduce abundance of HEI10 on diakinesis chromosomes**

266

267 Increased temperature influences MR rate by modulating type-I CO formation in Arabidopsis
268 (Modliszewski et al., 2018). Univalents in heat-stressed autotetraploid Col-0 plants suggested
269 a reduced CO rate under the high temperatures. To this end, we quantified the number of
270 HEI10 that acts in type-I CO formation pathway in diakinesis-staged meiocytes of
271 autotetraploid Col-0 plants. The plants grown under control temperature showed ~18.10
272 HEI10 foci per meiocyte (Fig. 5A and B); by contrast, the abundance of HEI10 reduced to
273 ~11.80 and ~0.56 per meiocyte in the plants stressed by 32°C and 37°C, respectively (Fig. 5A,
274 C and D), which suggested that the high temperatures significantly inhibited occurrence of
275 type-I class CO in the autotetraploid Col-0 plants.

276

277 **DSB formation in autotetraploid Arabidopsis is suppressed under high temperatures**

278

279 Generation of DSB is crucial for CO formation (De Muyt et al., 2007; Hartung et al., 2007;
280 Kurzbauer et al., 2012). To test whether heat-induced reduction of CO was owing to a
281 compromised DSB formation, like in diploid Arabidopsis (Ning et al., 2021), we quantified
282 the number of γ H2A.X, which specifically marks DSB sites, on zygotene chromosomes.
283 Under control temperature, an average of ~146.5 γ H2A.X foci per meiocyte was detected (Fig.
284 6A and D). In plants stressed by 32°C and 37°C, however, the abundance of γ H2A.X was
285 reduced to ~79.5 and ~84.8 per meiocyte, respectively (Fig. 6B-D), which indicated a
286 significantly lowered DSB formation. In support of this, the number of DMC1 that
287 specifically catalyzes DSB repair for MR was reduced to ~39.4 and ~49.7 per meiocyte under
288 32°C and 37°C, respectively, which were much lowered compared with control (~142) (Fig.
289 6E-H). These data provided evidence that high temperatures impose a negative impact on
290 DSB formation in autotetraploid Arabidopsis.

291

292 **Heat stress destabilizes ASY1 and ASY4 accumulation on chromosomes**

293

294 To reveal the impact of high temperature on chromosome axis formation in autotetraploid
295 Arabidopsis, we analyzed loading of the main axis-associated components; i.e. SYN1, ASY1
296 and ASY4 proteins in heat-stressed autotetraploid Col-0 plants. Under control temperature,
297 linear SYN1 and ASY1 signals overlapped and were fully associated with the entire zygotene
298 chromosomes (Fig. 7A). At late pachytene, when homologous chromosomes synapsed, ASY1
299 were unloaded at some chromosome regions (Fig. 7B). After heat treatment, although that
300 some zygotene chromosomes showed uninfluenced accumulation of ASY1 (Fig. 7C and D);

301 Supplement Fig. S5A, 19.55%; Supplement Fig. S6A), most zygotene and pachytene
302 chromosomes displayed dotted configuration of ASY1 (Fig. 7E and F, yellow arrows;
303 Supplement Fig. S5A, 80.45%; Supplement Fig. S6B-F), suggesting an impacted stability of
304 ASY1-associated axis. By contrast, no obvious alteration in SYN1 loading was observed in
305 heat-stressed meiocytes (Fig. 7C-F, I-K).

306

307 On the other hand, early zygotene chromosomes in autotetraploid Col-0 displayed thin linear
308 ASY4 loading (Supplement Fig. S7A), which was extended to the whole chromosomes from
309 middle zygotene to middle pachytene (Fig. 7G and H; Supplement Fig. S7B and C). As the
310 progressing of MR, ASY4 signals showed disassociation with some chromosome regions
311 from late pachytene (Supplement Fig. S7D), and were further unloaded at diplotene with
312 remaining dotted ASY4 foci on diakinesis-staged chromosomes (Supplement Fig. S7E-G). In
313 heat-stressed plants, a minor proportion of zygotene and pachytene chromosomes displayed
314 normal ASY4 accumulation (Fig. 7I; Supplement Fig. S5B, 19.85%; Supplement Fig. S7H
315 and I); on the contrary, a majority of zygotene- and pachytene-staged meiocytes showed
316 dotted ASY4 foci (Fig. 7J and K, yellow arrows; Supplement Fig. S5B, 80.15%; Supplement
317 Fig. S7J and K). Punctate ASY4 signals also occurred on the univalent chromosomes
318 (Supplement Fig. S7L). These findings suggested that heat stress specifically destabilizes the
319 ASY1- and ASY4- but not SYN1-mediated chromosome axis.

320

321 **Overlapped abnormalities of ASY1 and ASY4 in the *syn1* mutant**

322

323 It was proposed that assembly of ASY1-associated lateral element of SC relies on a step-wise
324 formation of SYN1-ASY3-mediated chromosome axis, which is bridged by ASY4 (Chambon
325 et al., 2018; Ferdous et al., 2012; Lambing et al., 2020b). To consolidate the role of ASY4 in
326 mediating ASY1 assembly, we performed co-immunostaining of ASY1 and ASY4 in the *syn1*
327 mutant. At middle zygotene, when homologous chromosomes partially paired and synapsed,
328 ASY1 and ASY4 were fully assembled along the whole chromosomes in the diploid Col-0
329 plants (Fig. 8A). By contrast, incomplete and/or fragmented ASY1 and ASY4 configuration
330 were observed in zygotene and pachytene meiocytes of the *syn1* mutant (Fig. 8B and C),
331 which, in addition, overlapped (Fig. 8B and C). This supported the notion that
332 ASY1-associated SC assembly relies on ASY4-mediated axis formation, which in turn
333 depends on functional SYN1.

334

335 Moreover, DSB formation is considered a downstream event of axis formation and occurs
336 independently of SC assembly (Lambing et al., 2020b; Sanchez-Moran et al., 2007). To
337 consolidate this model, we checked localization of ASY1 and ASY4 in the meiocytes of
338 *spo11-1-1*, *rad51* and *dmc1* mutants. We did not detect any alteration in loading of ASY1
339 and/or ASY4 on chromosomes of these mutants (Fig. 8D, *spo11-1-1*; E, *rad51* and F, *dmc1*).

340

341 **Co-localization of abnormal ASY1 and ASY4 signals on chromosomes of heat-stressed** 342 **diploid and autotetraploid Arabidopsis**

343

344 Considering the similarities of defective ASY1 and ASY4 accumulation under heat stress, and

345 the upstream action of axis formation on SC assembly (Fig. 7E and F, J and K; Fig. 8B and C)
346 (Ferdous et al., 2012; Lambing et al., 2020b; Ning et al., 2021), we hypothesized that heat
347 stress destabilizes ASY1-associated SC via impacted ASY4-mediated chromosome axis. To
348 this end, we conducted a combined staining of ASY1 and ASY4 in both the heat-stressed
349 diploid and autotetraploid Col-0 plants. Under control temperature, ASY1 and ASY4
350 co-localized on the entire chromosomes of diploid and autotetraploid Col-0 at early and
351 middle zygotene (Fig. 9A and D; Supplement Fig. S8A and B). ASY1 subsequently started to
352 be disassociated with the chromosomes from early to late pachytene, when ASY4 displayed
353 relatively stable linear configuration (Supplement Fig. S8C-E). Dotted ASY1 foci occurred at
354 diplotene, which became sparser at diakinesis representing a completed functioning of ASY1
355 in mediating homolog synapsis (Supplement Fig. S8F and G). ASY4, however, displayed a
356 slower unloading off the chromosomes, which supported its role in aiding the assembly of
357 ASY1 (Supplement Fig. S8F and G). Interestingly, in heat-stressed diploid and autotetraploid
358 Col-0 plants, incomplete and/or dotted ASY1 and ASY4 signals co-localized on the
359 chromosomes (Fig. 9B and C, E and F, yellow arrows). These observations favored the
360 hypothesis that heat stress destabilizes ASY1-associated SC via a compromised stability of
361 ASY4-mediated axis.

362

363 **Impaired ZYP1-dependent transverse filament under heat stress**

364

365 Formation of ZYP1-dependent transverse filament (TF) of SC is required for homolog
366 synapsis (Barakate et al., 2014; Capilla-Pérez et al., 2021; France et al., 2021; Higgins et al.,
367 2005; Wang et al., 2010). We analyzed ZYP1 assembly to examine the impact of heat stress
368 on the central element of SC in autotetraploid Col-0 plants. In control, ZYP1 proteins were
369 linearly and partially loaded at the central regions of paired homologous chromosomes from
370 zygotene (Fig. 10A), which were fully assembled at middle pachytene representing a matured
371 SC formation (Fig. 10B). As the disintegration of SC from late pachytene, ZYP1 proteins
372 were gradually disassociated with chromosomes (Fig. 10C). After heat treatment, dotted
373 and/or fragmented installation of ZYP1 on chromosomes were observed from early zygotene
374 to late pachytene (Fig. 10D-H, yellow arrow), indicating that assembly of transverse filament
375 of SC was impaired. Meanwhile, aggregated and/or enlarged ZYP1 foci implied pairing of
376 multiple chromosomes (Fig. 10D, G and H, blue arrows) (Morgan et al., 2017). Overall, these
377 figures suggested that heat stress disrupts the building of ZYP1-dependent transverse filament
378 of SC in autotetraploid Arabidopsis.

379

380 **Discussion**

381

382 WGD is a conserved phenomenon that contributes to genomic diversity and speciation in
383 higher plants (Comai, 2005; Dubcovsky and Dvorak, 2007; Ren et al., 2018; te Beest et al.,
384 2012; Van de Peer et al., 2020). Additional copies of genome, however, increase the
385 complexity for homologous chromosomes to pair and synapse (Lloyd and Bomblies, 2016;
386 Svačina et al., 2020; Yant et al., 2013). In our study, the autotetraploid Col-0 plants generate a
387 low but consistently-detectable rate (~4.53%) of aberrant meiotic products under normal

388 temperature conditions (Fig. 1, 2 and 3), suggesting that meiotic alterations naturally occur in
389 these autotetraploid *Arabidopsis* plants. The regularly formed spindle and phragmoplast
390 microtubule arrays in the autotetraploid Col-0 plants under control temperature (Fig. 3)
391 indicate that the meiotic defects are not caused by alterations in microtubular cytoskeleton
392 and cytokinesis, but are probably induced by the alterations in earlier meiosis processes, e.g.
393 improper chromosome behaviors with a resultant impacted CO formation. Chromosome
394 spreading analysis confirmed this which showed incomplete and/or irregular pairing and
395 synapsis at pachytene stage (Fig. 4B-D). The observation of regions of co-aligned, but
396 un-synapsed axes suggest that the synapsis defects are (or at least in part) independent of
397 defects in chromosome pairing (Capilla-Pérez et al., 2021; France et al., 2021). At the same
398 time, we found that the autotetraploid *Arabidopsis* plants primarily generate diakinesis PMCs
399 that contain five tetravalents (Fig. 4). This phenotype supports the opinion that autotetraploid
400 plants, in contrast to allotetraploids, preferentially undergo synapsis between four
401 homologous chromosomes (Braz et al., 2021; Lloyd and Bomblies, 2016; Svačina et al.,
402 2020). The unbalanced chromosome segregation at anaphase I could result from the
403 difficulties in multivalent resolving in the meiocytes with a mixed existence of tetravalents
404 and bivalents, as well as the ten bivalents (Yant et al., 2013). The autotetraploid Col-0 plants
405 that we used here was colchicine treatment-induced, which is very typical of newly formed
406 (neo)-autotetraploids that is believed to be less stable than the evolution-derived
407 autotetraploids; e.g. *A. lyrata* and *A. arenosa* (Henry et al., 2014; Lloyd and Bomblies, 2016;
408 Yant et al., 2013). Therefore, the meiotic defects we observed are probably the effects of
409 polyploidization without natural selection.

410

411 Under heat stress, as other plant species, the autotetraploid Col-0 plants exhibit a severe
412 organization of phragmoplast and RMAs at the end of meiosis (Fig. 3I, K and L), indicating
413 that microtubular cytoskeleton is a prominent targeted by high temperatures (De Storme and
414 Geelen, 2020; Lei et al., 2020; Mai et al., 2019; Wang et al., 2017). Nevertheless,
415 heat-induced polyad formation, and the disrupted RMA configuration could be a secondary
416 effort from the impaired spindle and/or a univalent-induced mis-segregation of chromatids at
417 MII, which normally occur in mutants with a defective MR (Bai et al., 1999; Shi et al., 2021;
418 Xue et al., 2019). Besides, in heat-stressed autotetraploid *Arabidopsis*, a high frequency of
419 univalents is induced and the abundance of HEI10 is lowered, indicating a largely suppressed
420 CO formation. Subsequent cytological analysis on key MR events suggested that the high
421 temperatures interfere with MR in the autotetraploid *Arabidopsis* plants probably by
422 impacting DSB formation, and by destabilizing chromosome axis and SC. Genome
423 duplication has been suggested to provide increased tolerance to environmental stresses (Folk
424 et al., 2020; Lourkisti et al., 2020; Rao et al., 2020). However, in contrast to the diploid
425 *Arabidopsis* Col-0 plants, we here showed that the neo-autotetraploid Col-0 generates a
426 higher frequency of aberrant meiotic products under high temperatures (Fig. 1; ~92.5% at
427 37°C) (Lei et al., 2020). Meanwhile, we recorded a higher rate of destabilized loading of
428 ASY1 and ASY4 in the heat-stressed autotetraploid Col-0 plants (80.45% defective ASY1 and
429 80.15% defective ASY4 in autotetraploid Col-0) (Ning et al., 2021), which represents
430 enhanced sensitivity of axis and SC formation to increased temperature. These facts suggest
431 that meiosis programs, especially for axis organization and chromosome dynamics are more

432 unstable under high temperatures in neo-tetraploid *Arabidopsis thaliana*.

433

434 The significantly reduced abundance of γ H2A.X and DMC1 in autotetraploid Col-0 plants
435 under high temperatures indicated an interfered DSB generation (Fig. 6). This phenomenon is
436 similar with what has been reported in the diploid *Arabidopsis* (Ning et al., 2021), which
437 suggests that a duplicated genome does not change the threshold of DSB formation system in
438 *Arabidopsis thaliana*. In *Saccharomyces cerevisiae*, DSB repair defect is more pronounced
439 under lower temperature (Pohl and Nickoloff, 2008). The negative impact of high
440 temperatures on DSB formation thus is likely conserved among eukaryotes. The attempt to
441 reveal how heat stress influences DSB formation has been tried by examining the expression
442 of key DSB generation-involved factors in the diploid *Arabidopsis*, which showed that the
443 transcripts of neither *SPO11-1* nor *PRD1*, 2 and 3 are sensitive to the increased temperature.
444 Therefore, heat stress induces DSB reduction not likely by impacting the DSB formation
445 machineries at the mRNA levels. In multiple species, the activity of phosphatidylinositol 3
446 kinase-like (PI3K) protein kinase Ataxia-Telangiectasia Mutated (ATM), which undertakes a
447 conserved function in sensing DNA damage and subsequently evoking DSB repair events
448 (reviewed by (Paull, 2015)), is negatively correlated with DSB abundance (Carballo et al.,
449 2013; Garcia et al., 2015; Joyce et al., 2011; Lange et al., 2011; Li and Yanowitz, 2019;
450 Mohibullah and Keeney, 2017; Zhang et al., 2011). A recent report in *Arabidopsis* suggested
451 that ATM limits DSB formation by restricting the accumulation of SPO11-1 on chromatin,
452 with the *atm* mutant having increased amount of SPO11-1 (Kurzbaue et al., 2021).
453 Supportively, the *atm* mutation increases the foci of recombinases RAD51 and DMC1;
454 meanwhile, it enhances the chromosome fragmentation in the *atcom1* mutant, which is
455 defective for DSB processing (Kurzbaue et al., 2021; Uanschou et al., 2007). We have
456 previously identified an elevated expression of *ATM* in heat-stressed diploid *Arabidopsis*
457 plants (Ning et al., 2021). Taken together, it is possible that high temperatures interfere with
458 DSB formation with associated induction of univalents by activating *ATM*. To this end, a
459 decreased SPO11-1 abundance should occur in heat-stressed wild-type plants, and the *atm*
460 mutant may exhibit higher DSB threshold to increased temperatures. Further examination on
461 SPO11 dynamics under increased temperature thus is of necessity to verify the hypothesis.

462

463 In both diploid and autotetraploid *Arabidopsis*, we observed an interfered configuration of
464 ASY1 and ASY4 on chromosomes (Fig. 7 and 9) (Ning et al., 2021). At the same time,
465 fragmented and/or disrupted ZYP1 loading, and multilayer-SC structures occurs in both the
466 diploid and autotetraploid *Arabidopsis* under high temperatures (Fig. 10) (Loidl, 1989;
467 Morgan et al., 2017; Ning et al., 2021). These facts reveal that chromosome axis and SC are
468 the prominent targets by high temperatures that interfere with MR. In the *syn1* mutant, the
469 accumulation of ASY3 and ASY4 is compromised, which, however, is not the case conversely
470 (Fig. 8) (Chambon et al., 2018; Ferdous et al., 2012; Lambing et al., 2020b). Considering that
471 a linear configuration of ASY3 depends on a functional ASY4 (Chambon et al., 2018), it is
472 possible that SYN1, ASY4 and ASY3 act in a stepwise manner in mediating axis formation.
473 However, since it has been evidenced by BiFC and Y2H assays that a direct interaction exists
474 between ASY4 and ASY3 (Chambon et al., 2018), we cannot exclude the possibility that the
475 normal loading of ASY4 also relies on the existence of ASY3 on the chromatin. Furthermore,

476 it has been shown that ASY1 cannot be regularly loaded onto chromosomes in plants depleted
477 with any of the axis-associated factors, which, however, in other way round are not impacted
478 in the *asy1* mutant (Chambon et al., 2018; Chelysheva et al., 2005; Ferdous et al., 2012;
479 Lambing et al., 2020a; Lambing et al., 2020b). This supports the notion that the assembly of
480 SC occurs downstream of axis formation. In line with this, we observed a delayed unloading
481 of ASY4 than ASY1 at later prophase I chromosomes (Supplement Fig. S8). Interestingly,
482 heat-destabilized ASY1 and ASY4 signals occur at a very close frequency, which additionally
483 co-localize on the chromosomes in both diploid and tetraploid *Arabidopsis* (Fig. 9) (Ning et
484 al., 2021). The instability of lateral element of SC under high temperatures therefore is
485 probably owing to an impacted axis formation. Since SYN1 keeps stable under the high
486 temperatures, it is plausible that heat stress specifically targets the ASY4 and/or
487 ASY3-mediated bridge structure that organizes and anchors the lateral element of SC to
488 chromosome axis. Whether the aggregated and/or dotted ASY1 and ASY4 loading are
489 somehow preferentially distributed at specific chromosome regions remain further
490 investigation.

491

492 **Supplemental materials**

493

494 The following files are available in the online version of this article.

495 Supplement Figure S1. FISH analysis of somatic cells in autotetraploid Col-0 plants.

496 Supplement Figure S2. Orcein staining of meiosis-staged flower buds in autotetraploid Col-0
497 plants stressed by 32°C.

498 Supplement Figure S3. Meiotic cell wall formation in heat-stressed autotetraploid Col-0
499 plants.

500 Supplement Figure S4. Meiotic spread of autotetraploid Col-0 plants.

501 Supplement Figure S5. Quantification of meiocytes with immunostaining of ASY1 and ASY4
502 in autotetraploid Col-0 plants.

503 Supplement Figure S6. Immunolocalization of ASY1 in meiocytes of autotetraploid Col-0
504 plants.

505 Supplement Figure S7. Immunolocalization of ASY4 in meiocytes of autotetraploid Col-0
506 plants.

507 Supplement Figure S8. Co-immunolocalization of ASY1 and ASY4 in meiocytes of
508 autotetraploid Col-0 plants.

509

510 **Materials and methods**

511

512 **Plant materials and growth conditions**

513

514 Autotetraploid and diploid *Arabidopsis thaliana* Columbia-0 (Col-0) plants, and the *syn1-1*
515 (SALK_137095), *rad51* (SAIL_873_C08), *spo11-1-1* (Grelon et al., 2001) and *dmc1*
516 (SALK_056177) (Sanchez-Moran et al., 2007) mutants were used in the study. The
517 autotetraploid Col-0 plants were generated as reported (De Storme and Geelen, 2011). Seeds

518 were germinated in soil for 6-8 days and seedlings were transferred to soil and cultivated with
519 a 16 h day/8 h night, 20°C, and 50% humidity condition. For temperature treatments, young
520 flowering plants were transferred to a humid chamber with a 16 h day/8 h night and incubated
521 at 32 and/or 37°C, respectively, for 24 h. All the treatment started from 8:00-10:00 AM.
522 Meiosis-staged flower buds were fixed by carnoy's fixative or paraformaldehyde upon the
523 finish of treatments.

524

525 **Generation of antibodies**

526

527 The anti-AtSYN1 antibodies were raised in rabbits by referring to (Bai et al., 1999); the
528 anti-AtASY1 antibodies were generated in rabbits and mice, respectively, against the
529 amino acid sequence SKAGNTPISNKAQPAASRES of AtASY1 conjugated to KLH; the
530 anti-AtZYP1 antibody (rat) was generated against the amino acid sequence
531 GSKRSEHIRVRSNDNVQD of AtZYP1 conjugated to KLH.

532

533 **Immunolocalization of MR proteins and α -tubulin**

534

535 Immunostaining of α -tubulin and MR proteins was performed as reported (Chelysheva et al.,
536 2010; Liu et al., 2017; Wang et al., 2014). Antibodies against ZYP1 (rabbit and/or rat) (Ning
537 et al., 2020), DMC1 (rabbit) (Ning et al., 2020) and γ H2A.X (rabbit) (Lambing et al., 2020b)
538 were diluted by 1:100; antibodies against α -tubulin (rat) (Lei et al., 2020), ASY1 (rabbit
539 and/or mouse), ASY4 (rabbit) (Ning et al., 2020) and SYN1 (mouse) were diluted by 1:200;
540 antibody against CENH3 (rabbit) (Abcam, 72001) was diluted by 1:400; antibody against
541 SYN1 (rabbit) was diluted by 1:500. The secondary antibodies; i.e. Goat anti-Rabbit IgG
542 (H+L) Cross-Adsorbed Secondary Antibody Alexa Fluor 555 (Invitrogen, A32732), Goat
543 anti-Rabbit IgG (H+L) Highly Cross-Adsorbed Secondary Antibody Alexa Fluor Plus 488
544 (Invitrogen, A32731), Goat anti-Rat IgG (H+L) Cross-Adsorbed Secondary Antibody, Alexa
545 Fluor 555 (Invitrogen, A21434), Goat anti-Rat IgG (H+L) Cross-Adsorbed Secondary
546 Antibody, Alexa Fluor 488 (Invitrogen, A11006) and Goat anti-Mouse IgG (H+L) Highly
547 Cross-Adsorbed Secondary Antibody, Alexa Fluor Plus 488 (Invitrogen, A32723) were
548 diluted to 10 μ g/mL.

549

550 **Cytology and fluorescence in situ hybridization**

551

552 Meiotic chromosome behaviors were analyzed by performing chromosome spreading using
553 meiosis-staged flower buds fixed at least 24 h by carnoy's fixative. Flower buds were washed
554 twice by distilled water and once in citrate buffer (10 mM, pH = 4.5), and were incubated in
555 digestion enzyme mixture (0.3% pectolyase, 0.3% cellulase and 0.3% cytohelicase) in citrate
556 buffer (10 mM, pH = 4.5) at 37°C in a moisture chamber for 2.5-3.5 h. Subsequently, 6-8
557 digested buds were washed in distilled water, and were transferred to a glass slide squashed in
558 a small amount (4-5 μ L) of distilled water followed by adding two rounds of 10 μ L precooled
559 60% acetic acid. The samples were stirred gently on a hotplate at 45°C for 1-2 min, which
560 thereafter was flooded with precooled carnoy's fixative. The slides were subsequently air
561 dried for 10 min, and were stained by adding 8 μ L DAPI (10 μ g/mL) in Vectashield antifade

562 mounting medium, mounted with a coverslip, and sealed by nail polish. Tetrad analysis by
563 orcein and/or aniline blue staining was performed by referring to (Lei et al., 2020; Ning et al.,
564 2021). FISH assay was performed by referring to (Lei et al., 2020).

565

566 **Microscopy and quantification of fluorescent foci**

567

568 Bright-field images and DAPI-stained meiotic chromosomes were pictured using a M-Shot
569 ML31 microscope equipped with a MS60 camera. Aniline blue staining of meiotic cell walls,
570 and immunolocalization of α -tubulin and MR-related proteins were analyzed on an Olympus
571 IX83 inverted fluorescence microscope equipped with a X-Cite lamp and a Prime BSI camera.
572 Image processing and quantification of fluorescent foci were conducted as previously
573 reported (Ning et al., 2021).

574

575 **Author contribution**

576

577 H.Q.F. performed most of the experiments; K.Y., X.H.Z. and J.Y.Z. performed meiotic spread
578 analysis; E.I.E. performed FISH experiment; H.L., J.X., C.L.C. and G.H.Y. contributed to
579 data analysis; C.W. analyzed γ H2A.X and DMC1 foci; B.L. conceived the project, analyzed
580 data, and wrote the manuscript.

581

582 **Funding**

583

584 This work was supported by National Natural Science Foundation of China (32000245 to
585 B.L.), Hubei Provincial Natural Science Foundation of China (2020CFB159 to B.L.),
586 Fundamental Research Funds for the Central Universities, South-Central University for
587 Nationalities (CZY20001 to B.L.), Fundamental Research Funds for the Central Universities,
588 South-Central University for Nationalities (YZZ18007 to B.L.), National Natural Science
589 Foundation of China (31900261 to C.W.), National Natural Science Foundation of China
590 (31270361 to G.H.Y.), Fundamental Research Funds for the Central Universities (CZZ21004
591 to G.H.Y.), and National Natural Science Foundation of China (31971525 to C.L.C.).

592

593 **Acknowledgement**

594

595 The authors thank Dr. Jing Li (Huazhong Agricultural University) and Dr. Yingxiang Wang
596 (Fudan University) for kindly providing the autotetraploid Col-0 seeds, and the anti-HEI10
597 (rabbit) antibody, respectively. They appreciate Dr. Wojtek Pawlowski (Cornell University)
598 for the discussion and suggestions while collecting data. Especially, the authors appreciate Dr.
599 Andrew Lloyd (IBERS) for critical review and comments on the manuscript prior to
600 submission.

601

602 **Interest of conflict**

603

604 All the authors declared that there is no conflict of interest in this work.

605

606 **References**

607

608 **Armstrong, S.J., Caryl, A.P., Jones, G.H., and Franklin, F.C.** (2002). Asy1, a protein required
609 for meiotic chromosome synapsis, localizes to axis-associated chromatin in
610 Arabidopsis and Brassica. *J Cell Sci* **115**, 3645-3655.

611 **Bai, X., Peirson, B.N., Dong, F., Xue, C., and Makaroff, C.A.** (1999). Isolation and
612 Characterization of SYN1, a RAD21-like Gene Essential for Meiosis in Arabidopsis.
613 *Plant Cell* **11**, 417-430.

614 **Barakate, A., Higgins, J.D., Vivera, S., Stephens, J., Perry, R.M., Ramsay, L., Colas, I., Oakey,**
615 **H., Waugh, R., Franklin, F.C., Armstrong, S.J., and Halpin, C.** (2014). The
616 synaptonemal complex protein ZYP1 is required for imposition of meiotic crossovers
617 in barley. *Plant Cell* **26**, 729-740.

618 **Berchowitz, L.E., Francis, K.E., Bey, A.L., and Copenhaver, G.P.** (2007). The role of AtMUS81
619 in interference-insensitive crossovers in *A. thaliana*. *Plos Genetics* **3**, e132.

620 **Bergerat, A., de Massy, B., Gadelle, D., Varoutas, P.-C., Nicolas, A., and Forterre, P.** (1997).
621 An atypical topoisomerase II from archaea with implications for meiotic recombination.
622 *Nature* **386**, 414-417.

623 **Bhatt, A.M., Canales, C., and Dickinson, H.G.** (2001). Plant meiosis: the means to 1N. *Trends*
624 in *Plant Science* **6**, 114-121.

625 **Bomblies, K., Higgins, J.D., and Yant, L.** (2015). Meiosis evolves: adaptation to external and

- 626 internal environments. *New Phytologist* **208**, 306-323.
- 627 **Bombles, K., Jones, G., Franklin, C., Zickler, D., and Kleckner, N.** (2016). The challenge of
628 evolving stable polyploidy: could an increase in "crossover interference distance" play
629 a central role? *Chromosoma* **125**, 287-300.
- 630 **Braz, G.T., Yu, F., Zhao, H., Deng, Z., Birchler, J.A., and Jiang, J.** (2021). Preferential meiotic
631 chromosome pairing among homologous chromosomes with cryptic sequence
632 variation in tetraploid maize. *New Phytologist* **229**, 3294-3302.
- 633 **Bretagnolle, F., and Thompson, J.D.** (1995). Gametes with the somatic chromosome number:
634 mechanisms of their formation and role in the evolution of autopolyploid plants. *New*
635 *Phytologist* **129**, 1-22.
- 636 **Cai, X., Dong, F., Edelman, R.E., and Makaroff, C.A.** (2003). The Arabidopsis SYN1 cohesin
637 protein is required for sister chromatid arm cohesion and homologous chromosome
638 pairing. *J Cell Sci* **116**, 2999-3007.
- 639 **Capilla-Pérez, L., Durand, S., Hurel, A., Lian, Q., Chambon, A., Taochy, C., Solier, V., Grelon,**
640 **M., and Mercier, R.** (2021). The synaptonemal complex imposes crossover
641 interference and heterochiasmy in Arabidopsis. *Proc Natl Acad Sci U S A* **118**,
642 e2023613118.
- 643 **Carballo, J.A., Panizza, S., Serrentino, M.E., Johnson, A.L., Geymonat, M., Borde, V., Klein,**
644 **F., and Cha, R.S.** (2013). Budding yeast ATM/ATR control meiotic double-strand
645 break (DSB) levels by down-regulating Rec114, an essential component of the
646 DSB-machinery. *Plos Genetics* **9**, e1003545.
- 647 **Chambon, A., West, A., Vezon, D., Horlow, C., De Muyt, A., Chelysheva, L., Ronceret, A.,**

- 648 **Darbyshire, A., Osman, K., Heckmann, S., Franklin, F.C.H., and Grelon, M.** (2018).
649 Identification of ASYNAPTIC4, a component of the meiotic chromosome axis. *Plant*
650 *Physiology* **178**, 233-246.
- 651 **Chelysheva, L., Grandont, L., Vrielynck, N., Guin, S.I., Mercier, R., and Grelon, M.** (2010). An
652 easy protocol for studying chromatin and recombination protein dynamics during
653 *Arabidopsis thaliana* meiosis: immunodetection of cohesins, histones and MLH1.
654 *Cytogenetic and Genome Research* **129**, 143-153.
- 655 **Chelysheva, L., Diallo, S., Vezon, D., Gendrot, G., Vrielynck, N., Belcram, K., Rocques, N.,**
656 **Márquez-Lema, A., Bhatt, A.M., Horlow, C., Mercier, R., Mézard, C., and Grelon, M.**
657 (2005). AtREC8 and AtSCC3 are essential to the monopolar orientation of the
658 kinetochores during meiosis. *Journal of Cell Science* **118**, 4621-4632.
- 659 **Cloud, V., Chan, Y.L., Grubb, J., Budke, B., and Bishop, D.K.** (2012). Rad51 is an accessory
660 factor for Dmc1-mediated joint molecule formation during meiosis. *Science* **337**,
661 1222-1225.
- 662 **Comai, L.** (2005). The advantages and disadvantages of being polyploid. *Nat Rev Genet* **6**,
663 836-846.
- 664 **Da Ines, O., Degroote, F., Goubely, C., Amiard, S., Gallego, M.E., and White, C.I.** (2013).
665 Meiotic recombination in *Arabidopsis* is catalysed by DMC1, with RAD51 playing a
666 supporting role. *Plos Genetics* **9**, e1003787.
- 667 **Da Ines, O., Michard, R., Fayos, I., Bastianelli, G., Nicolas, A., Guiderdoni, E., White, C., and**
668 **Sourdille, P.** (2020). Bread wheat TaSPO11-1 exhibits evolutionarily conserved
669 function in meiotic recombination across distant plant species. *Plant Journal* **103**,

- 670 2052-2068.
- 671 **De Muyt, A., Vezon, D., Gendrot, G., Gallois, J.-L., Stevens, R., and Grelon, M. (2007).**
672 AtPRD1 is required for meiotic double strand break formation in *Arabidopsis thaliana*.
673 EMBO Journal **26**, 4126-4137.
- 674 **De Storme, N., and Geelen, D. (2011).** The *Arabidopsis* mutant *jason* produces unreduced first
675 division restitution male gametes through a parallel/fused spindle mechanism in
676 meiosis II. Plant Physiology **155**, 1403-1415.
- 677 **De Storme, N., and Geelen, D. (2013).** Cytokinesis in plant male meiosis. Plant Signaling &
678 Behavior **8**, e23394.
- 679 **De Storme, N., and Geelen, D. (2014).** The impact of environmental stress on male
680 reproductive development in plants: biological processes and molecular mechanisms.
681 Plant Cell and Environment **37**, 1-18.
- 682 **De Storme, N., and Geelen, D. (2020).** High temperatures alter cross-over distribution and
683 induce male meiotic restitution in *Arabidopsis thaliana*. Communications Biology **3**,
684 187.
- 685 **De Storme, N., Copenhaver, G.P., and Geelen, D. (2012).** Production of diploid male gametes
686 in *Arabidopsis* by cold-induced destabilization of postmeiotic radial microtubule arrays.
687 Plant Physiology **160**, 1808-1826.
- 688 **Del Pozo, J.C., and Ramirez-Parra, E. (2015).** Whole genome duplications in plants: an
689 overview from *Arabidopsis*. Journal of Experimental Botany **66**, 6991-7003.
- 690 **Draeger, T., and Moore, G. (2017).** Short periods of high temperature during meiosis prevent
691 normal meiotic progression and reduce grain number in hexaploid wheat (*Triticum*

- 692 aestivum L.). Theoretical and Applied Genetics **130**, 1785-1800.
- 693 **Dubcovsky, J., and Dvorak, J.** (2007). Genome plasticity a key factor in the success of
694 polyploid wheat under domestication. Science **316**, 1862-1866.
- 695 **Ferdous, M., Higgins, J.D., Osman, K., Lambing, C., Roitinger, E., Mechtler, K., Armstrong,**
696 **S.J., Perry, R., Pradillo, M., Cuñado, N., and Franklin, F.C.H.** (2012). Inter-homolog
697 crossing-over and synapsis in Arabidopsis meiosis are dependent on the chromosome
698 axis protein AtASY3. Plos Genetics **8**, e1002507-e1002507.
- 699 **Folk, R.A., Siniscalchi, C.M., and Soltis, D.E.** (2020). Angiosperms at the edge: extremity,
700 diversity, and phylogeny. Plant Cell and Environment **43**, 2871-2893.
- 701 **France, M.G., Enderle, J., Röhrig, S., Puchta, H., Franklin, F.C.H., and Higgins, J.D.** (2021).
702 ZYP1 is required for obligate cross-over formation and cross-over interference in
703 Arabidopsis. Proc Natl Acad Sci U S A **118**.
- 704 **Garcia, V., Gray, S., Allison, R.M., Cooper, T.J., and Neale, M.J.** (2015). Tel1ATM-mediated
705 interference suppresses clustered meiotic double-strand-break formation. Nature **520**,
706 114-118.
- 707 **Grandont, L., Cuñado, N., Coriton, O., Huteau, V., Eber, F., Chèvre, A.M., Grelon, M.,**
708 **Chelysheva, L., and Jenczewski, E.** (2014). Homoeologous chromosome sorting and
709 progression of meiotic recombination in Brassica napus: ploidy does matter! Plant Cell
710 **26**, 1448-1463.
- 711 **Grelon, M., Vezon, D., Gendrot, G., and Pelletier, G.** (2001). AtSPO11-1 is necessary for
712 efficient meiotic recombination in plants. Embo j **20**, 589-600.
- 713 **Hartung, F., Wurz-Wildersinn, R., Fuchs, J., Schubert, I., Suer, S., and Puchta, H.** (2007). The

714 catalytically active tyrosine residues of both SPO11-1 and SPO11-2 are required for
715 meiotic double-strand break induction in Arabidopsis. *Plant Cell* **19**, 3090-3099.

716 **Henry, I.M., Dilkes, B.P., Tyagi, A., Gao, J., Christensen, B., and Comai, L.** (2014). The BOY
717 NAMED SUE quantitative trait locus confers increased meiotic stability to an adapted
718 natural allopolyploid of Arabidopsis. *Plant Cell* **26**, 181-194.

719 **Higgins, J.D., Armstrong, S.J., Franklin, F.C.H., and Jones, G.H.** (2004). The Arabidopsis
720 MutS homolog AtMSH4 functions at an early step in recombination: evidence for two
721 classes of recombination in Arabidopsis. *Genes & Development* **18**, 2557-2570.

722 **Higgins, J.D., Sanchez-Moran, E., Armstrong, S.J., Jones, G.H., and Franklin, F.C.** (2005).
723 The Arabidopsis synaptonemal complex protein ZYP1 is required for chromosome
724 synapsis and normal fidelity of crossing over. *Genes & Development* **19**, 2488-2500.

725 **Hollingsworth, N.M., and Brill, S.J.** (2004). The Mus81 solution to resolution: generating
726 meiotic crossovers without Holliday junctions. *Genes & Development* **18**, 117-125.

727 **Jackson, S., and Chen, Z.J.** (2010). Genomic and expression plasticity of polyploidy. *Current*
728 *Opinion in Plant Biology* **13**, 153-159.

729 **Joyce, E.F., Pedersen, M., Tiong, S., White-Brown, S.K., Paul, A., Campbell, S.D., and McKim,**
730 **K.S.** (2011). *Drosophila* ATM and ATR have distinct activities in the regulation of
731 meiotic DNA damage and repair. *Journal of Cell Biology* **195**, 359-367.

732 **Kim, J., and Choi, K.** (2019). Signaling-mediated meiotic recombination in plants. *Current*
733 *Opinion in Plant Biology* **51**, 44-50.

734 **Klimyuk, V.I., and Jones, J.D.G.** (1997). AtDMC1, the Arabidopsis homologue of the yeast
735 DMC1 gene: characterization, transposon-induced allelic variation and

- 736 meiosis-associated expression. *Plant Journal* **11**, 1-14.
- 737 **Kobayashi, W., Liu, E., Ishii, H., Matsunaga, S., Schlogelhofer, P., and Kurumizaka, H. (2019).**
738 Homologous pairing activities of *Arabidopsis thaliana* RAD51 and DMC1. *J Biochem*
739 **165**, 289-295.
- 740 **Kurzbauer, M.-T., Janisiw, M.P., Paulin, L.F., Prusén Mota, I., Tomanov, K., Krsicka, O.,**
741 **Haeseler, A.v., Schubert, V., and Schlögelhofer, P. (2021).** ATM controls meiotic DNA
742 double-strand break formation and recombination and affects synaptonemal complex
743 organization in plants. *The Plant Cell*.
- 744 **Kurzbauer, M.T., Uanschou, C., Chen, D., and Schlogelhofer, P. (2012).** The recombinases
745 DMC1 and RAD51 are functionally and spatially separated during meiosis in
746 *Arabidopsis*. *Plant Cell* **24**, 2058-2070.
- 747 **Lambing, C., Kuo, P.C., Tock, A.J., Topp, S.D., and Henderson, I.R. (2020a).** ASY1 acts as a
748 dosage-dependent antagonist of telomere-led recombination and mediates crossover
749 interference in *Arabidopsis*. *Proc Natl Acad Sci U S A* **117**, 13647-13658.
- 750 **Lambing, C., Tock, A.J., Topp, S.D., Choi, K., Kuo, P.C., Zhao, X., Osman, K., Higgins, J.D.,**
751 **Franklin, F.C.H., and Henderson, I.R. (2020b).** Interacting genomic landscapes of
752 REC8-cohesin, chromatin, and meiotic recombination in *Arabidopsis*. *Plant Cell* **32**,
753 1218-1239.
- 754 **Lan, W.-H., Lin, S.-Y., Kao, C.-Y., Chang, W.-H., Yeh, H.-Y., Chang, H.-Y., Chi, P., and Li,**
755 **H.-W. (2020).** Rad51 facilitates filament assembly of meiosis-specific Dmc1
756 recombinase. *Proc Natl Acad Sci U S A* **117**, 11257-11264.
- 757 **Lange, J., Pan, J., Cole, F., Thelen, M.P., Jasin, M., and Keeney, S. (2011).** ATM controls

- 758 meiotic double-strand-break formation. *Nature* **479**, 237-240.
- 759 **Lei, X., Ning, Y., Eid Elesawi, I., Yang, K., Chen, C., Wang, C., and Liu, B.** (2020). Heat stress
760 interferes with chromosome segregation and cytokinesis during male meiosis in
761 *Arabidopsis thaliana*. *Plant Signaling & Behavior* **15**, 1746985.
- 762 **Leitch, A.R., and Leitch, I.J.** (2008). Genomic plasticity and the diversity of polyploid plants.
763 *Science* **320**, 481-483.
- 764 **Li, W., and Yanowitz, J.L.** (2019). ATM and ATR influence meiotic crossover formation through
765 antagonistic and overlapping functions in *Caenorhabditis elegans*. *Genetics* **212**,
766 431-443.
- 767 **Li, W., Chen, C., Markmann-Mulisch, U., Timofejeva, L., Schmelzer, E., Ma, H., and Reiss, B.**
768 (2004). The *Arabidopsis* *AtRAD51* gene is dispensable for vegetative development but
769 required for meiosis. *Proc Natl Acad Sci U S A* **101**, 10596-10601.
- 770 **Liu, B., De Storme, N., and Geelen, D.** (2017). Cold interferes with male meiotic cytokinesis in
771 *Arabidopsis thaliana* independently of the *AHK2/3-AHP2/3/5* cytokinin signaling
772 module. *Cell Biology International* **41**, 879-889.
- 773 **Liu, B., De Storme, N., and Geelen, D.** (2018). Cold-induced male meiotic restitution in
774 *Arabidopsis thaliana* is not mediated by GA-DELLA signaling. *Frontiers in Plant*
775 *Science* **9**, 91.
- 776 **Liu, B., Mo, W.J., Zhang, D., De Storme, N., and Geelen, D.** (2019). Cold influences male
777 reproductive development in plants: a hazard to fertility, but a window for evolution.
778 *Plant Cell Physiology* **60**, 7-18.
- 779 **Lloyd, A., and Bomblies, K.** (2016). Meiosis in autopolyploid and allopolyploid *Arabidopsis*.

- 780 Current Opinion in Plant Biology **30**, 116-122.
- 781 **Lloyd, A., Morgan, C., H. Franklin, F.C., and Bomblies, K.** (2018). Plasticity of Meiotic
782 Recombination Rates in Response to Temperature in Arabidopsis. *Genetics* **208**,
783 1409-1420.
- 784 **Lohani, N., Singh, M.B., and Bhalla, P.L.** (2019). High temperature susceptibility of sexual
785 reproduction in crop plants. *Journal of Experimental Botany* **71**, 555-568.
- 786 **Loidl, J.** (1989). Effects of elevated temperature on meiotic chromosome synapsis in *Allium*
787 *ursinum*. *Chromosoma* **97**, 449-458.
- 788 **Lourkisti, R., Froelicher, Y., Herbette, S., Morillon, R., Tomi, F., Gibernau, M., Giannettini, J.,**
789 **Berti, L., and Santini, J.** (2020). Triploid citrus genotypes have a better tolerance to
790 natural chilling conditions of photosynthetic capacities and specific leaf volatile organic
791 compounds. *Frontiers in Plant Science* **11**.
- 792 **Mai, Y., Li, H., Suo, Y., Fu, J., Sun, P., Han, W., Diao, S., and Li, F.** (2019). High temperature
793 treatment generates unreduced pollen in persimmon (*Diospyros kaki* Thunb.). *Scientia*
794 *Horticulturae* **258**, 108774.
- 795 **Modliszewski, J.L., Wang, H., Albright, A.R., Lewis, S.M., Bennett, A.R., Huang, J., Ma, H.,**
796 **Wang, Y., and Copenhaver, G.P.** (2018). Elevated temperature increases meiotic
797 crossover frequency via the interfering (Type I) pathway in *Arabidopsis thaliana*. *Plos*
798 *Genetics* **14**, e1007384.
- 799 **Mohibullah, N., and Keeney, S.** (2017). Numerical and spatial patterning of yeast meiotic DNA
800 breaks by Tel1. *Genome Research* **27**, 278-288.
- 801 **Morgan, C., Zhang, H., Henry, C.E., Franklin, F.C.H., and Bomblies, K.** (2020). Derived alleles

- 802 of two axis proteins affect meiotic traits in autotetraploid *Arabidopsis arenosa*. Proc
803 Natl Acad Sci U S A **117**, 8980-8988.
- 804 **Morgan, C.H., Zhang, H., and Bomblies, K.** (2017). Are the effects of elevated temperature on
805 meiotic recombination and thermotolerance linked via the axis and synaptonemal
806 complex? *Philos Trans R Soc Lond B Biol Sci* **372**, 20160470.
- 807 **Ning, Y., Liu, Q., Wang, C., Qin, E., Wu, Z., Wang, M., Yang, K., Elesawi, I.E., Chen, C., Liu,**
808 **H., Qin, R., and Liu, B.** (2020). Heat stress interferes with formation of double-strand
809 breaks and homolog synapsis in *Arabidopsis thaliana*. *BioRxiv*,
810 2020.2010.2002.324269.
- 811 **Ning, Y., Liu, Q., Wang, C., Qin, E., Wu, Z., Wang, M., Yang, K., Elesawi, I.E., Chen, C., Liu,**
812 **H., Qin, R., and Liu, B.** (2021). Heat stress interferes with formation of double-strand
813 breaks and homolog synapsis. *Plant Physiology*.
- 814 **Osman, K., Yang, J., Roitinger, E., Lambing, C., Heckmann, S., Howell, E., Cuacos, M., Imre,**
815 **R., Durnberger, G., Mechtler, K., Armstrong, S., and Franklin, F.C.H.** (2018). Affinity
816 proteomics reveals extensive phosphorylation of the *Brassica* chromosome axis
817 protein ASY1 and a network of associated proteins at prophase I of meiosis. *Plant*
818 *Journal* **93**, 17-33.
- 819 **Otto, S.P.** (2007). The evolutionary consequences of polyploidy. *Cell* **131**, 452-462.
- 820 **Parisod, C., Holderegger, R., and Brochmann, C.** (2010). Evolutionary consequences of
821 autopolyploidy. *New Phytologist* **186**, 5-17.
- 822 **Paull, T.T.** (2015). Mechanisms of ATM activation. *Annu Rev Biochem* **84**, 711-738.
- 823 **Pohl, T.J., and Nickoloff, J.A.** (2008). Rad51-independent interchromosomal double-strand

824 break repair by gene conversion requires Rad52 but not Rad55, Rad57, or Dmc1.
825 Molecular and cellular biology **28**, 897-906.

826 **Ramsey, J., and Schemske, D.W.** (1998). Pathways, mechanisms, and rates of polyploid
827 formation in flowering plants. Annual Review of Ecology and Systematics **29**, 467-501.

828 **Ramsey, J., and Schemske, D.W.** (2002). Neopolyploidy in flowering plants. Annual Review of
829 Ecology and Systematics **33**, 589-639.

830 **Rao, S., Tian, Y., Xia, X., Li, Y., and Chen, J.** (2020). Chromosome doubling mediates superior
831 drought tolerance in *Lycium ruthenicum* via abscisic acid signaling. Horticulture Res **7**, 40.

832 **Ren, R., Wang, H.F., Guo, C.C., Zhang, N., Zeng, L.P., Chen, Y.M., Ma, H., and Qi, J.** (2018).
833 Widespread whole genome duplications contribute to genome complexity and species
834 diversity in angiosperms. Molecular Plant **11**, 414-428.

835 **Sanchez-Moran, E., Santos, J.L., Jones, G.H., and Franklin, F.C.** (2007). ASY1 mediates
836 AtDMC1-dependent interhomolog recombination during meiosis in *Arabidopsis*.
837 Genes & Development **21**, 2220-2233.

838 **Santos, J.L., Alfaro, D., Sanchez-Moran, E., Armstrong, S.J., Franklin, F.C.H., and Jones, G.H.**
839 (2003). Partial diploidization of meiosis in autotetraploid *Arabidopsis thaliana*.
840 Genetics **165**, 1533-1540.

841 **Seear, P.J., France, M.G., Gregory, C.L., Heavens, D., Schmickl, R., Yant, L., and Higgins,**
842 **J.D.** (2020). A novel allele of ASY3 is associated with greater meiotic stability in
843 autotetraploid *Arabidopsis lyrata*. Plos Genetics **16**, e1008900-e1008900.

844 **Shahid, S.** (2020). The rules of attachment: REC8 cohesin connects chromatin architecture
845 and recombination machinery in meiosis. Plant Cell **32**, 808-809.

- 846 **Shi, W., Ji, J., Xue, Z., Zhang, F., Miao, Y., Yang, H., Tang, D., Du, G., Li, Y., Shen, Y., and**
847 **Cheng, Z.** (2021). PRD1, a homologous recombination initiation factor, is involved in
848 spindle assembly in rice meiosis. *New Phytologist* **230**, 585-600.
- 849 **Singh, G., Da Ines, O., Gallego, M.E., and White, C.I.** (2017). Analysis of the impact of the
850 absence of RAD51 strand exchange activity in Arabidopsis meiosis. *Plos One* **12**,
851 e0183006.
- 852 **Soltis, P.S., and Soltis, D.E.** (2009). The role of hybridization in plant speciation. *Annual*
853 *Review of Plant Biology* **60**, 561-588.
- 854 **Soltis, P.S., Marchant, D.B., Van de Peer, Y., and Soltis, D.E.** (2015). Polyploidy and genome
855 evolution in plants. *Current Opinion in Genetics & Development* **35**, 119-125.
- 856 **Stacey, N.J., Kuromori, T., Azumi, Y., Roberts, G., Breuer, C., Wada, T., Maxwell, A., Roberts,**
857 **K., and Sugimoto-Shirasu, K.** (2006). Arabidopsis SPO11-2 functions with SPO11-1 in
858 meiotic recombination. *Plant Journal* **48**, 206-216.
- 859 **Stift, M., Berenos, C., Kuperus, P., and van Tienderen, P.H.** (2008). Segregation models for
860 disomic, tetrasomic and intermediate inheritance in tetraploids: a general procedure
861 applied to rorippa (Yellow Cress) microsatellite data. *Genetics* **179**, 2113-2123.
- 862 **Su, H., Cheng, Z., Huang, J., Lin, J., Copenhaver, G.P., Ma, H., and Wang, Y.** (2017).
863 Arabidopsis RAD51, RAD51C and XRCC3 proteins form a complex and facilitate
864 RAD51 localization on chromosomes for meiotic recombination. *Plos Genetics* **13**,
865 e1006827.
- 866 **Sugimoto-Shirasu, K., Stacey, N.J., Corsar, J., Roberts, K., and McCann, M.C.** (2002). DNA
867 topoisomerase VI is essential for endoreduplication in Arabidopsis. *Curr Biol* **12**,

- 868 1782-1786.
- 869 **Svačina, R., Sourdille, P., Kopecký, D., and Bartoš, J.** (2020). Chromosome pairing in
870 polyploid grasses. *Frontiers in Plant Science* **11**, 1056.
- 871 **Tang, Z., Zhang, L., Yang, D., Zhao, C., and Zheng, Y.** (2011). Cold stress contributes to
872 aberrant cytokinesis during male meiosis I in a wheat thermosensitive genic male
873 sterile line. *Plant Cell and Environment* **34**, 389-405.
- 874 **te Beest, M., Le Roux, J.J., Richardson, D.M., Brysting, A.K., Suda, J., Kubesová, M., and
875 Pysek, P.** (2012). The more the better? The role of polyploidy in facilitating plant
876 invasions. *Ann Bot* **109**, 19-45.
- 877 **Uanschou, C., Siwec, T., Pedrosa-Harand, A., Kerzendorfer, C., Sanchez-Moran, E.,
878 Novatchkova, M., Akimcheva, S., Woglar, A., Klein, F., and Schlögelhofer, P.** (2007).
879 A novel plant gene essential for meiosis is related to the human CtIP and the yeast
880 COM1/SAE2 gene. *EMBO Journal* **26**, 5061-5070.
- 881 **Van de Peer, Y., Ashman, T.-L., Soltis, P.S., and Soltis, D.E.** (2020). Polyploidy: an
882 evolutionary and ecological force in stressful times. *Plant Cell* **33**, 11-26.
- 883 **Wang, J., Li, D., Shang, F., and Kang, X.** (2017). High temperature-induced production of
884 unreduced pollen and its cytological effects in *Populus*. *Scientific Reports* **7**, 5281.
- 885 **Wang, M., Wang, K., Tang, D., Wei, C., Li, M., Shen, Y., Chi, Z., Gu, M., and Cheng, Z.** (2010).
886 The central element protein ZEP1 of the synaptonemal complex regulates the number
887 of crossovers during meiosis in rice. *Plant Cell* **22**, 417-430.
- 888 **Wang, Y., and Copenhaver, G.P.** (2018). Meiotic recombination: mixing it up in plants. *Annual
889 Review of Plant Biology* **69**, 577-609.

- 890 **Wang, Y., Cheng, Z., Lu, P., Timofejeva, L., and Ma, H.** (2014). Molecular cell biology of male
891 meiotic chromosomes and isolation of male meiocytes in *Arabidopsis thaliana*.
892 *Methods Mol Biol* **1110**, 217-230.
- 893 **Wu, S., Han, B., and Jiao, Y.** (2020). Genetic contribution of paleopolyploidy to adaptive
894 evolution in angiosperms. *Molecular Plant* **13**, 59-71.
- 895 **Xue, M., Wang, J., Jiang, L., Wang, M., Wolfe, S., Pawlowski, W.P., Wang, Y., and He, Y.**
896 (2018). The number of meiotic double-strand breaks influences crossover distribution
897 in *Arabidopsis*. *Plant Cell* **30**, 2628-2638.
- 898 **Xue, Z., Liu, C., Shi, W., Miao, Y., Shen, Y., Tang, D., Li, Y., You, A., Xu, Y., Chong, K., and**
899 **Cheng, Z.** (2019). OsMTOPIVIB is required for meiotic bipolar spindle assembly. *Proc*
900 *Natl Acad Sci U S A* **116**, 15967-15972.
- 901 **Yant, L., Hollister, J.D., Wright, K.M., Arnold, B.J., Higgins, J.D., Franklin, F.C.H., and**
902 **Bomblies, K.** (2013). Meiotic adaptation to genome duplication in *Arabidopsis arenosa*.
903 *Current Biology* **23**, 2151-2156.
- 904 **Yao, Y., Li, X., Chen, W., Liu, H., Mi, L., Ren, D., Mo, A., and Lu, P.** (2020). ATM Promotes
905 RAD51-Mediated Meiotic DSB Repair by Inter-Sister-Chromatid Recombination in
906 *Arabidopsis*. *Frontiers in Plant Science* **11**, 839.
- 907 **Yin, Y., Cheong, H., Friedrichsen, D., Zhao, Y., Hu, J., Mora-Garcia, S., and Chory, J.** (2002).
908 A crucial role for the putative *Arabidopsis* topoisomerase VI in plant growth and
909 development. *Proc Natl Acad Sci U S A* **99**, 10191-10196.
- 910 **Zamariola, L., Tiang, C.L., De Storme, N., Pawlowski, W., and Geelen, D.** (2014).
911 Chromosome segregation in plant meiosis. *Frontiers in Plant Science* **5**, 279.

- 912 **Zhang, L., Kim, K.P., Kleckner, N.E., and Storlazzi, A.** (2011). Meiotic double-strand breaks
913 occur once per pair of (sister) chromatids and, via Mec1/ATR and Tel1/ATM, once per
914 quartet of chromatids. Proceedings of the National Academy of Sciences of the United
915 States of America **108**, 20036-20041.
- 916 **Zickler, D., and Kleckner, N.** (1999). Meiotic chromosomes: integrating structure and function.
917 Annu Rev Genet **33**, 603-754.
918

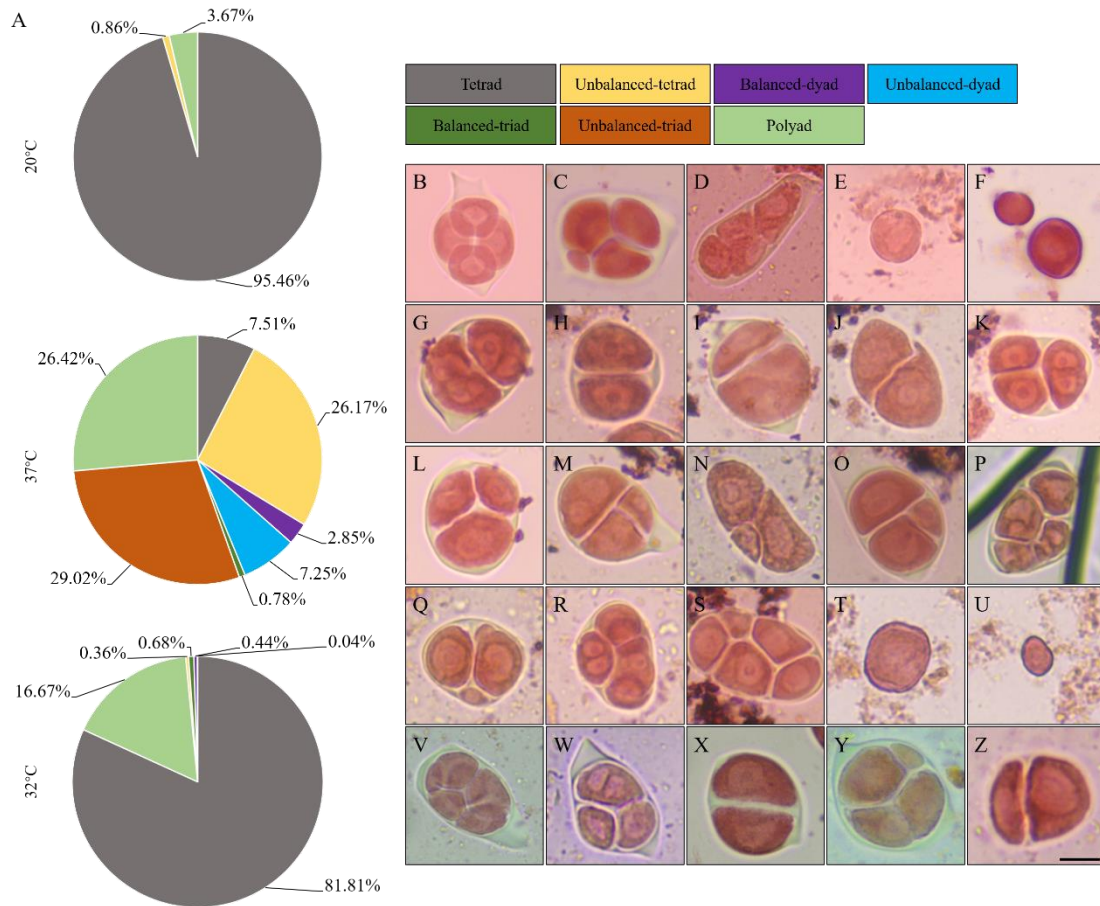


Figure 1. Tetrad analysis in heat-stressed autotetraploid Col-0 plants. A, Graph showing the frequency of tetrad-staged meiotic products in autotetraploid Col-0 plants incubated under 20°C, 32°C and 37°C, respectively. The numbers indicate the frequency of different types of tetrad-staged meiocytes. B-F, Tetrad-staged PMCs (B-D) and unicellular-staged microspores (E and F) of autotetraploid Col-0 plants grown under 20°C. G-U, Tetrad-staged PMCs (G-S) and unicellular-staged microspores (T and U) of autotetraploid Col-0 plants stressed by 37°C. V-Z, Tetrad-staged PMCs from autotetraploid Col-0 plants stressed by 32°C. Scale bar = 10 μ m.

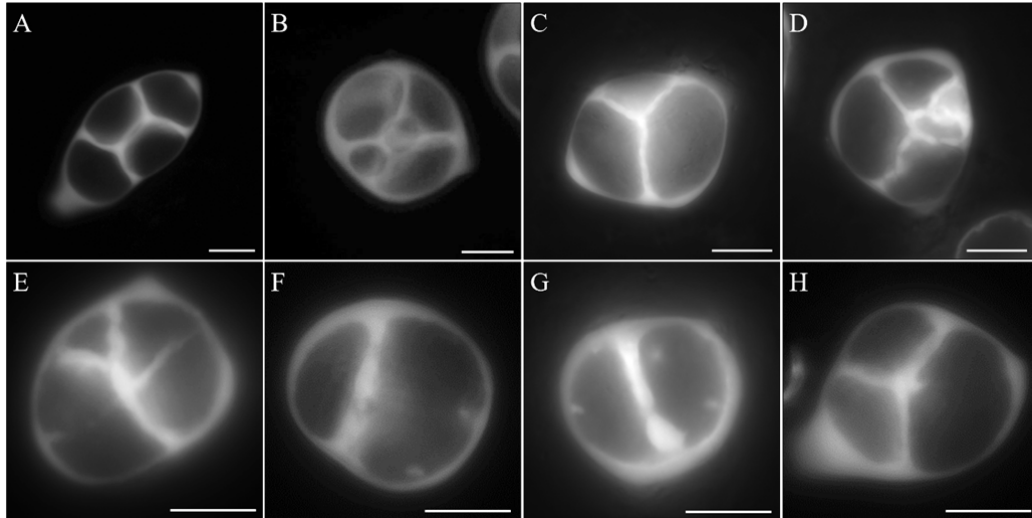


Figure 2. Meiotic cell wall formation in heat-stressed autotetraploid Col-0 plants. A-H, Aniline blue-stained callosic cell walls in autotetraploid Col-0 plants incubated under control (A and B) and high temperature (C-H). Scale bars = 10 μ m.

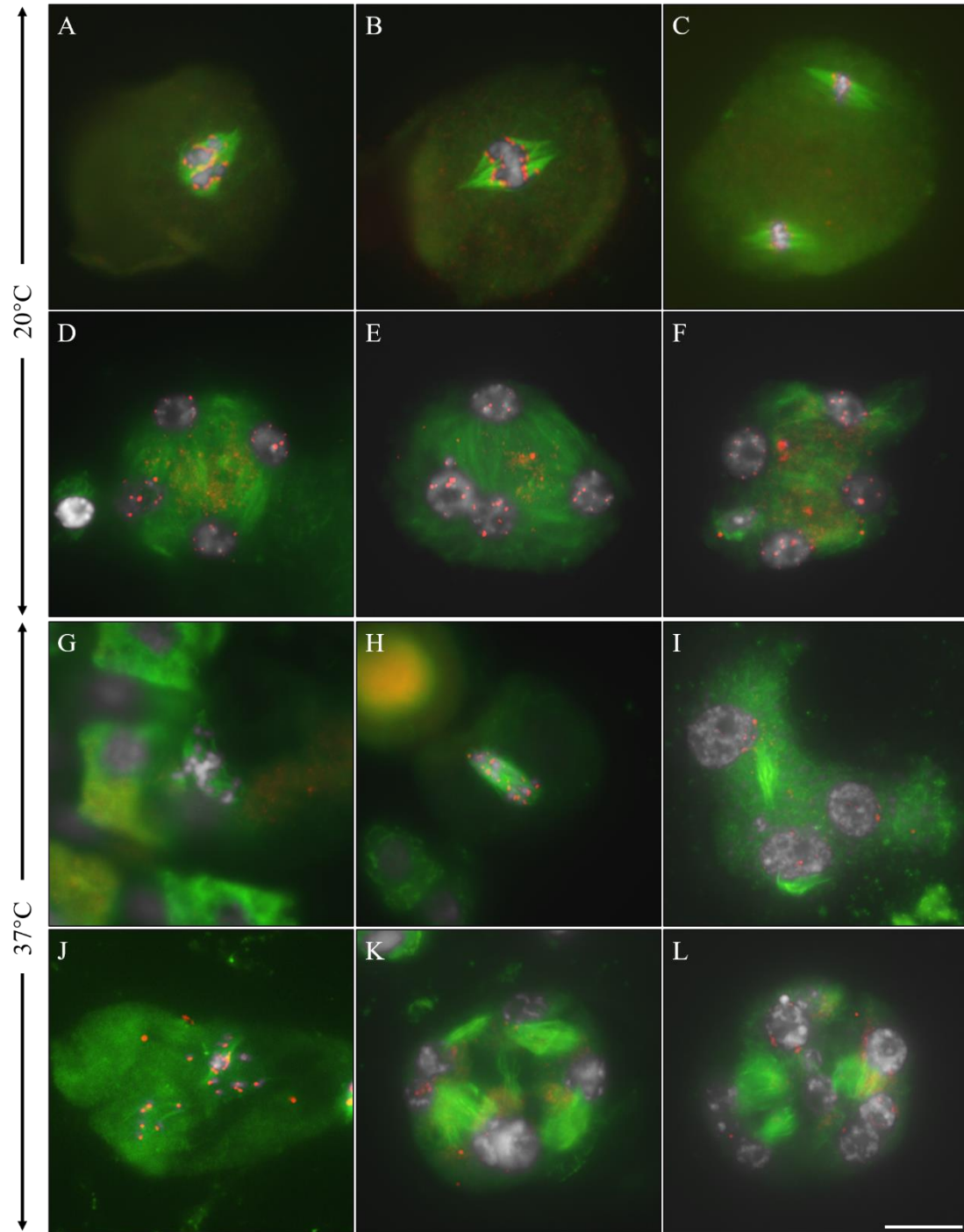


Figure 3. Microtubular cytoskeleton in meiocytes of autotetraploid Col-0 plants. A-F, Metaphase I- (A and B), metaphase II- (C) and telophase II-staged (D-F) PMCs in autotetraploid Col-0 plants under control temperature. G-L, Metaphase I- (G and H), interkinesis- (I), metaphase II- (J) and telophase II-staged (K and L) PMCs in autotetraploid Col-0 plants under high temperature. White, DAPI; green, α -tubulin; red, CENH3. Scale bar = 10 μ m.

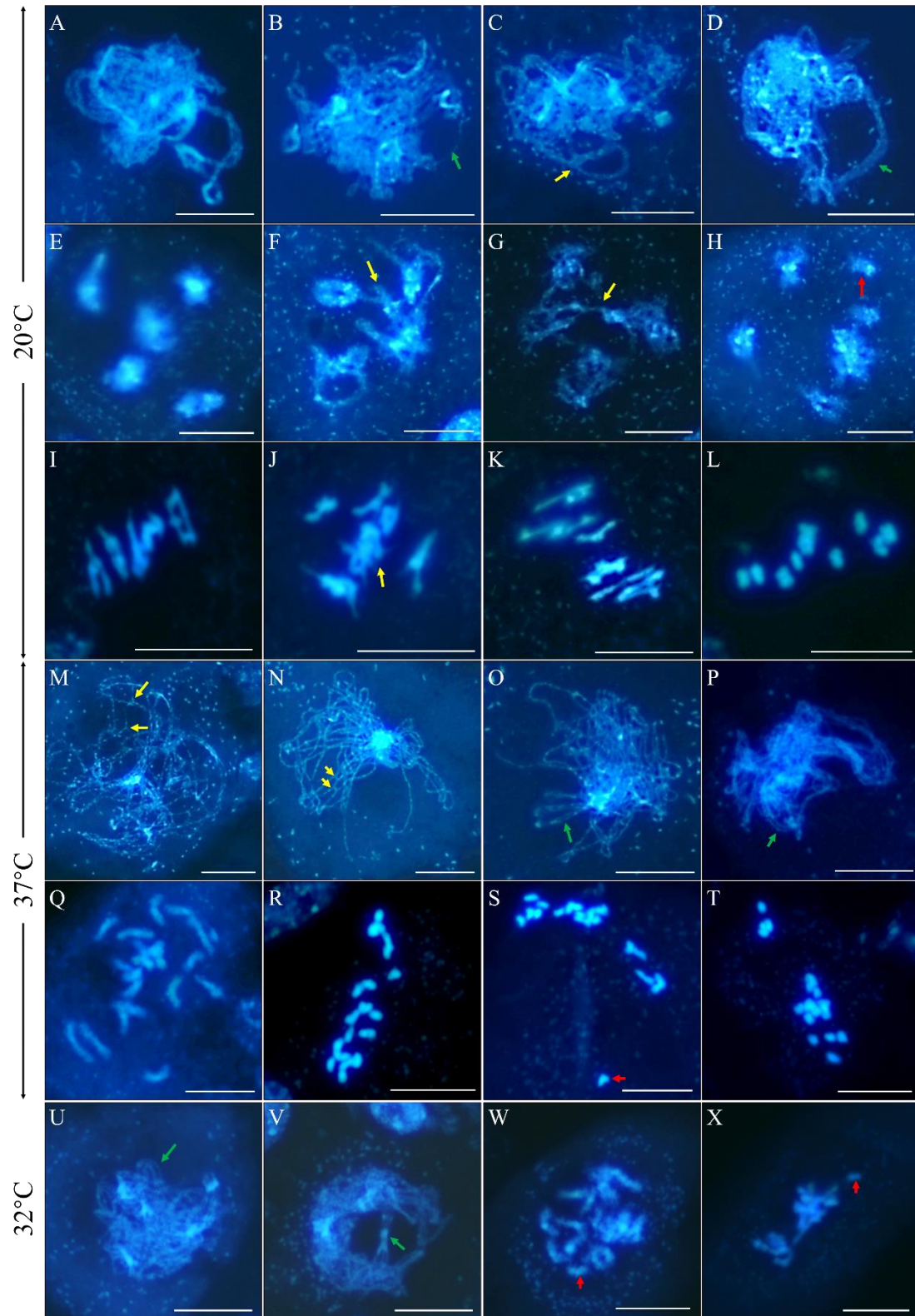


Figure 4. Chromosome behaviors in meiocytes of autotetraploid Col-0 plants. A-L, Chromosome spreading of Pachytene- (A-D), diakinesis- (E-H) and metaphase I-staged (I-L) meiocytes in autotetraploid Col-0 plants grown under control temperature. M-T, Chromosome spreading of zygotene- (M and N), pachytene- (O and P), diakinesis- (Q) and metaphase I-staged (R-T) meiocytes in autotetraploid Col-0 plants stressed by 37°C. U-X, Chromosome spreading of pachytene- (U and V),

diakinesis- (W) and metaphase I-staged (X) meiocytes in autotetraploid Col-0 plants stressed by 32°C. Green arrows indicate incomplete and/or abnormal pairing of chromosomes; yellow arrows indicate abnormal chromosome interactions; and red arrows indicate bivalents, univalents and/or lagged chromosomes. Scale bars = 10 μ m.

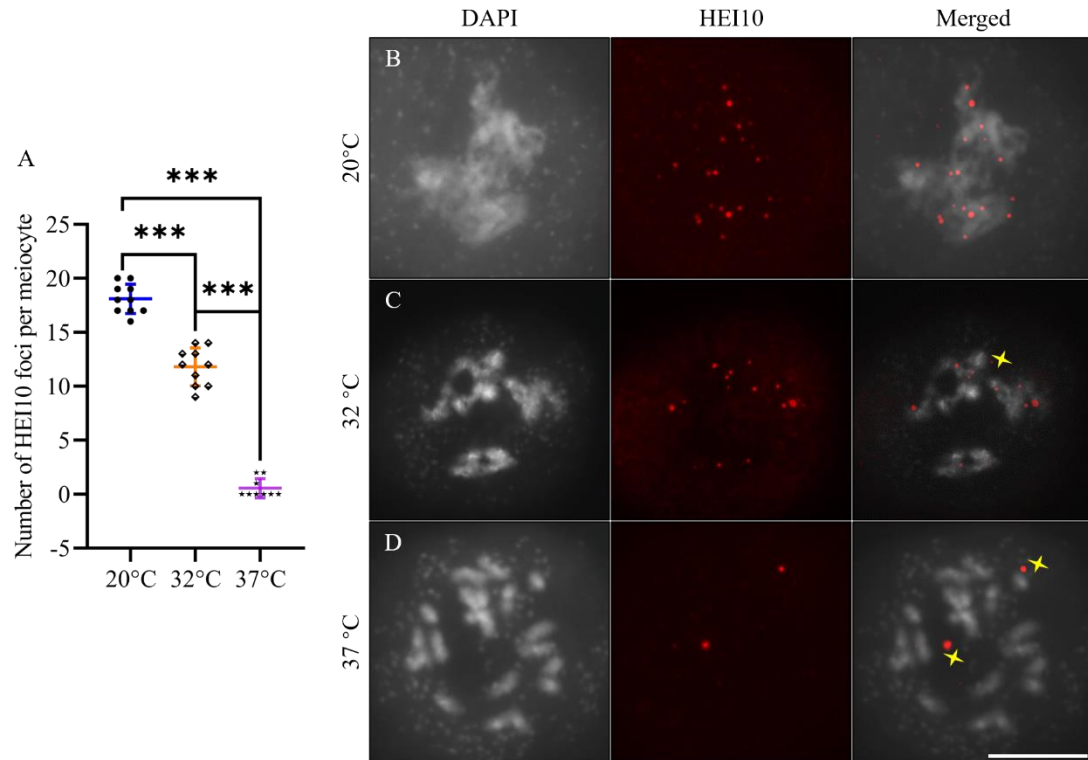


Figure 5. Localization of HEI10 on diakinesis chromosomes in autotetraploid Col-0 plants. A, Graph showing the number of HEI10 foci per diakinesis-staged meiocyte. One-way ANOVA test was performed, and the significance level was set as $P < 0.05$. *** indicates $P < 0.0001$. B-D, Immunolocalization of HEI10 on diakinesis chromosomes of autotetraploid Col-0 plants incubated under 20°C (B), 32°C (C) and 37°C (D), respectively. The yellow stars indicate non-specific foci to HEI10. Scale bar = 10 μm .

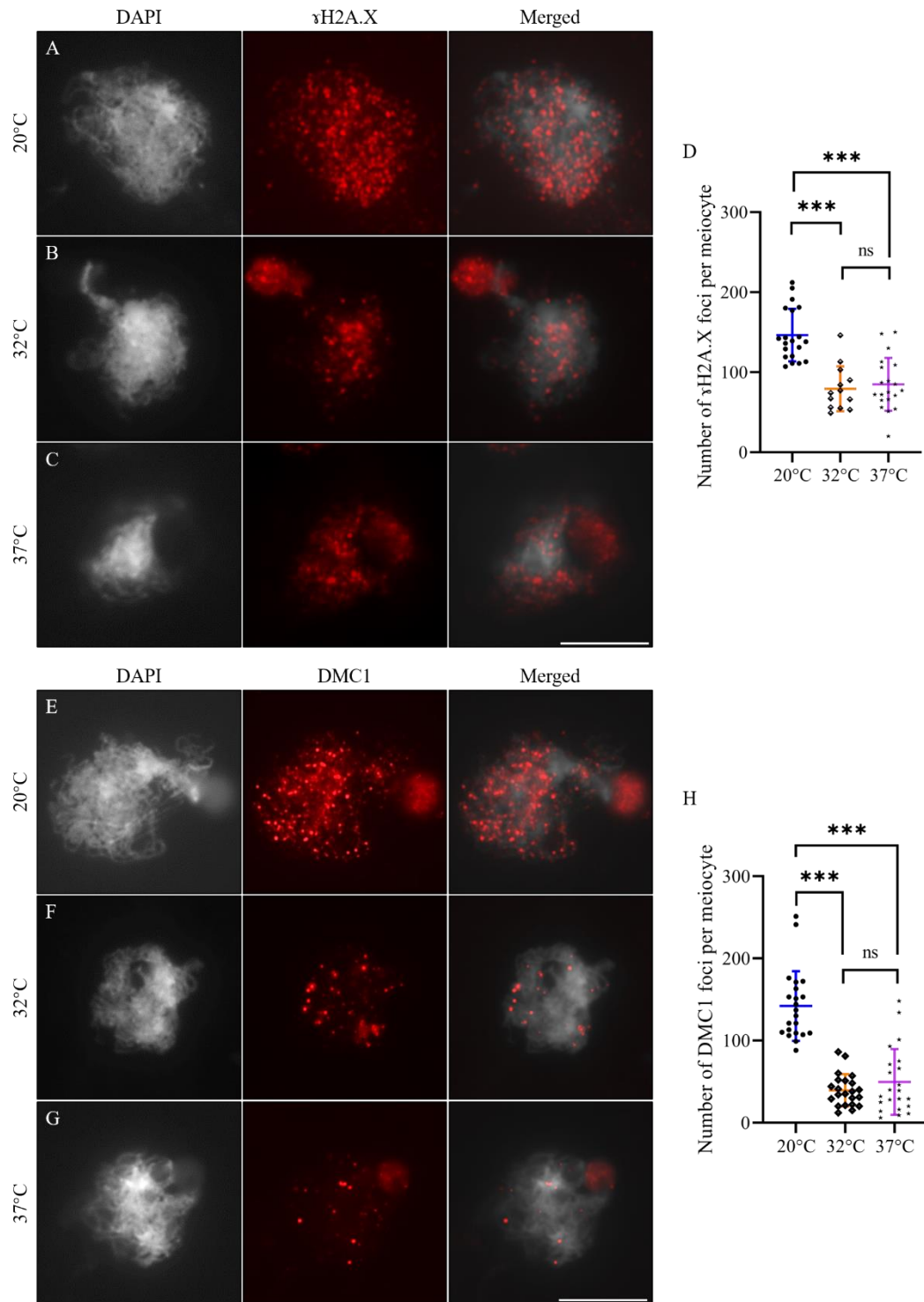


Figure 6. Heat stress reduces abundance of γ H2A.X and DMC1 on zygotene chromosomes. A-C, Immunolocalization of γ H2A.X on zygotene chromosomes of autotetraploid Col-0 plants under 20°C (A), 32°C (B) and 37°C (C), respectively. D, Graph showing the number of γ H2A.X foci per meiocyte in autotetraploid Col-0 plants under 20°C, 32°C and 37°C. E-G, Immunolocalization of DMC1 on zygotene chromosomes of autotetraploid Col-0 plants under 20°C (E), 32°C (F) and 37°C (G), respectively. H, Graph showing the number of DMC1 foci per meiocyte in autotetraploid Col-0 plants under 20°C, 32°C and 37°C. One-way ANOVA test was performed, and the significance level was set as $P < 0.05$. *** indicates $P < 0.001$; ns indicates $P > 0.05$. Scale bars = 10 μ m.

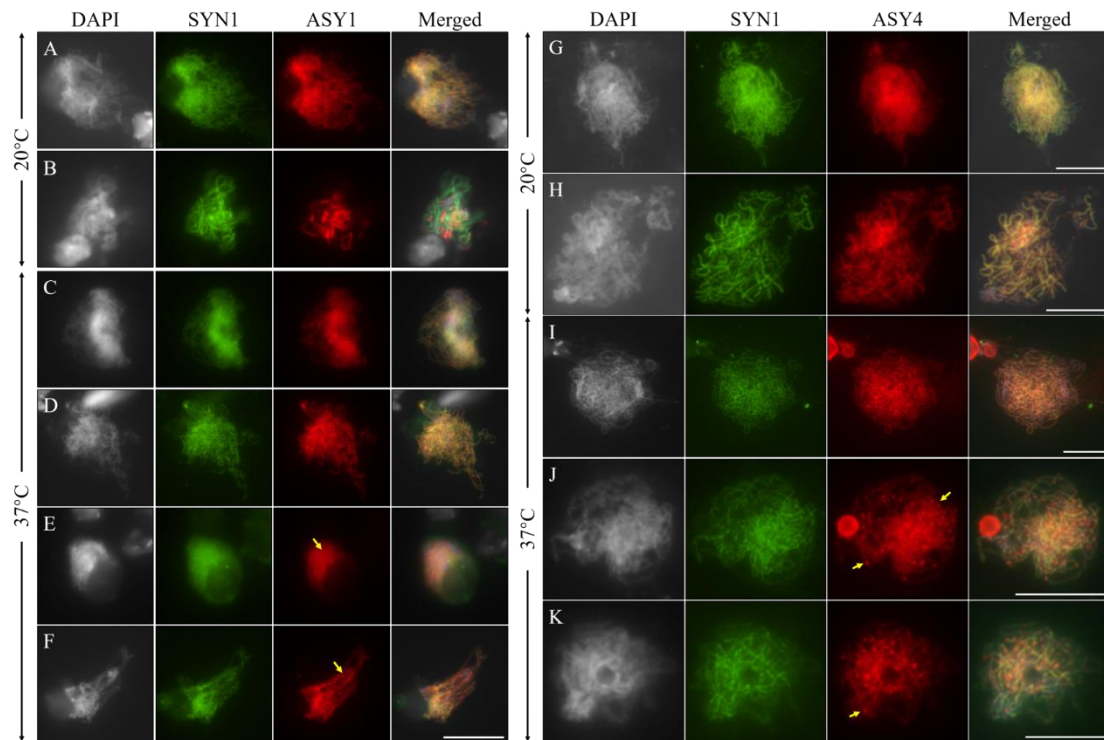


Figure 7. Immunostaining of chromosome axis components in meiocytes of autotetraploid Col-0 plants. A and B, Co-immunostaining of SYN1 and ASY1 on zygotene (A) and pachytene (B) chromosomes in control plants. C-F, Co-immunostaining of SYN1 and ASY1 on zygotene (C-E) and pachytene (F) chromosomes in heat-stressed plants. G and H, Co-immunostaining of SYN1 and ASY4 on zygotene (G) and pachytene (H) chromosomes in control plants. I-K, Co-immunostaining of SYN1 and ASY4 on zygotene (I and J) and pachytene (K) chromosomes in heat-stressed plants. Yellow arrows indicate dotted ASY1 and ASY4 foci. Scale bars = 10 μ m.

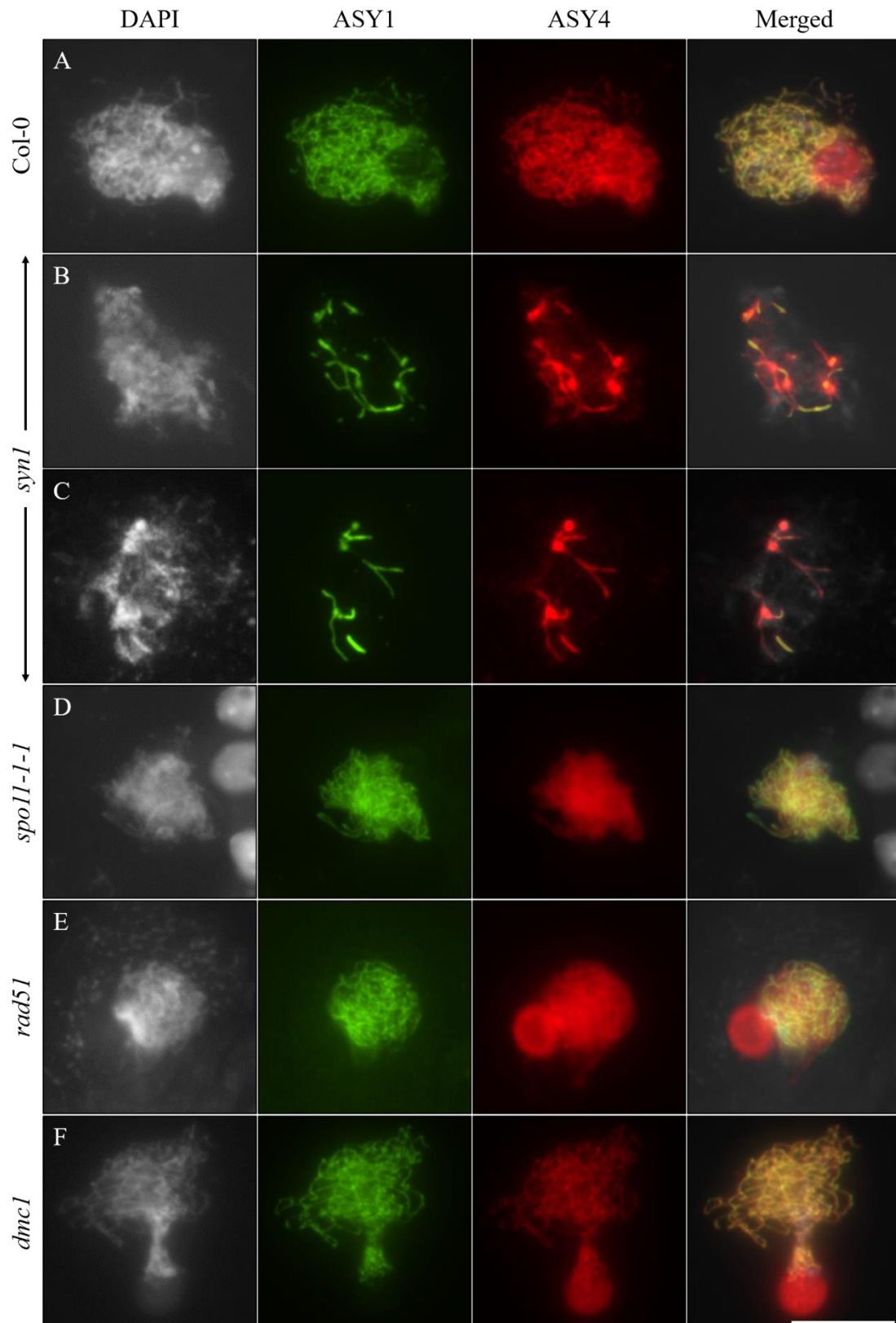


Figure 8. Immunostaining of ASY1 and ASY4 in meiotic chromosomes of diploid *Arabidopsis thaliana* plants. A-F, Immunolocalization of ASY1 and ASY4 on prophase I chromosomes of diploid Col-0 plants (A), and the *syn1* (B and C), *spoil-1-1* (D), *rad51* (E) and *dmc1* (F) mutants. Scale bar = 10 μ m.

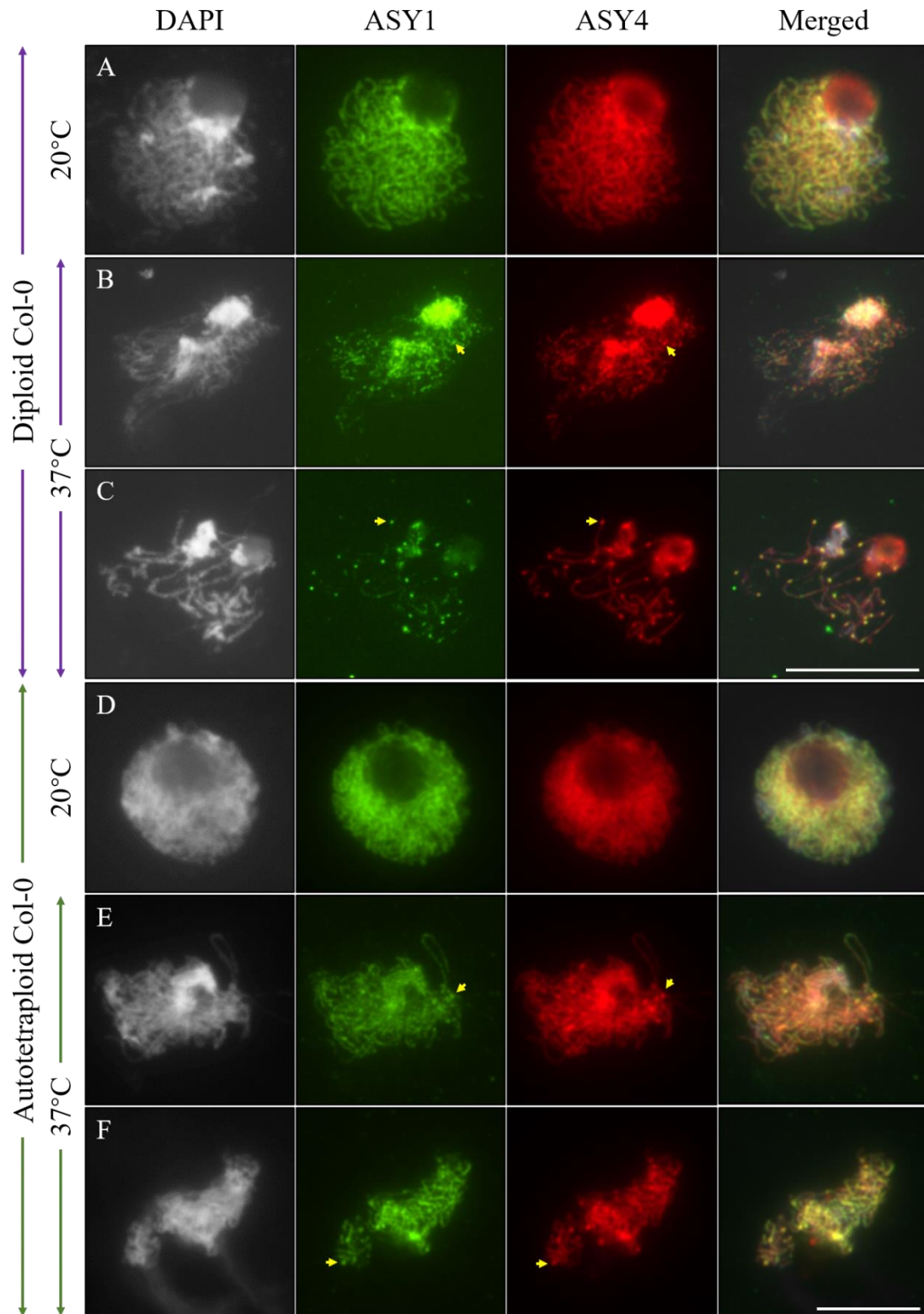


Figure 9. Co-localization of ASY1 and ASY4 in heat-stressed diploid and autotetraploid Col-0 plants. A and D, Zygotene-staged meiocytes in diploid (A) and autotetraploid (D) Col-0 plants grown under control temperature. B and C, Zygotene- (B) and pachytene-staged (C) meiocytes in heat-stressed diploid Col-0 plants. E and F, Zygotene- (E) and pachytene-staged (F) meiocytes in heat-stressed autotetraploid Col-0 plants. Yellow arrows indicate co-localization of dotted ASY1 and ASY4 foci.

Scale bars = 10 μm .

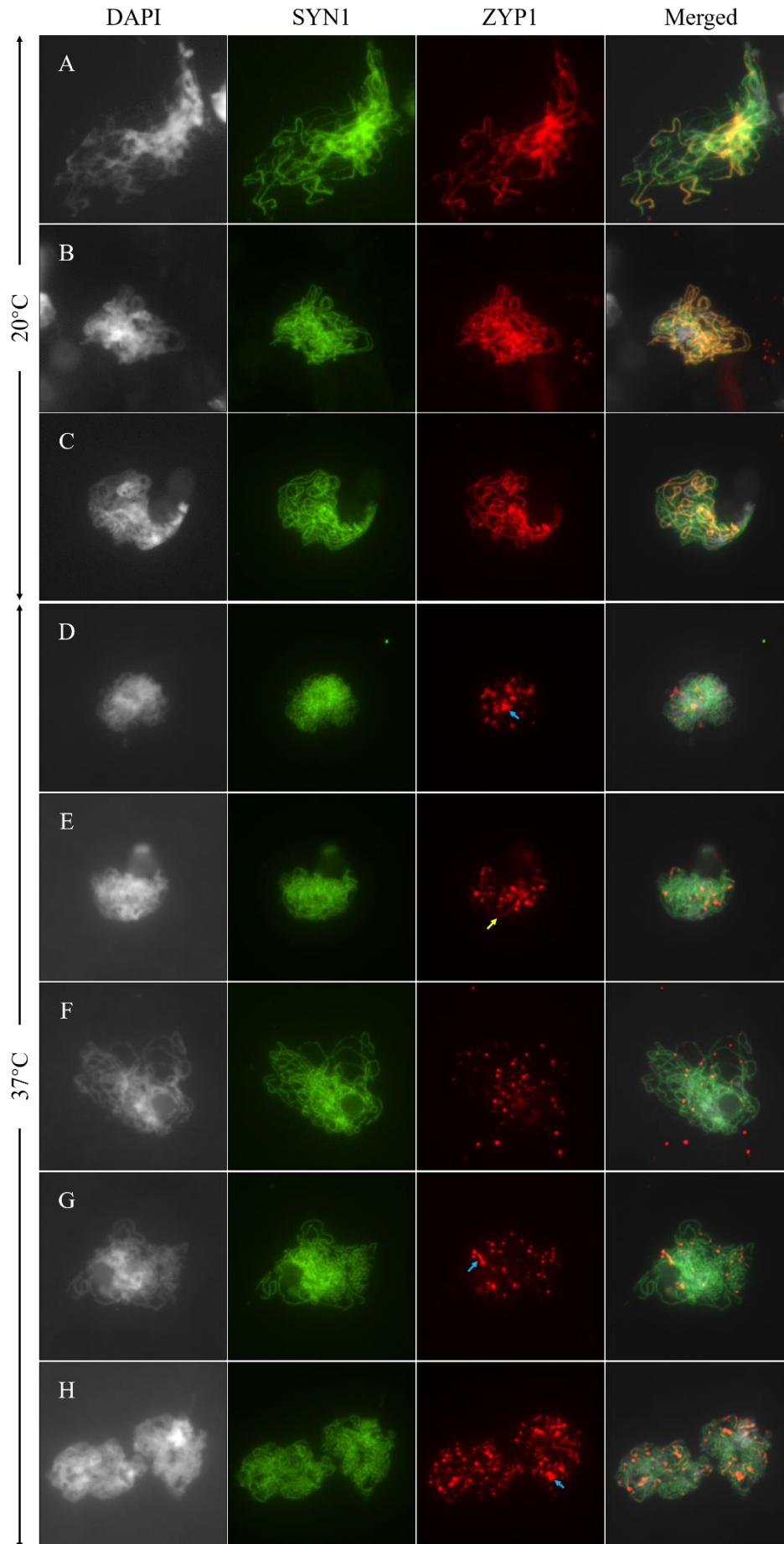


Figure 10. Immunolocalization of SYN1 and ZYP1 in meiocytes of autotetraploid Col-0 plants. A-C, Zygotene- (A), middle pachytene- (B) and late pachytene-staged (C) meiocytes in control plants. D-H, Early zygotene- (D), middle zygotene- (E), late zygotene- (F), middle pachytene- (G) and late pachytene-staged (H) meiocytes in heat-stress plants. Yellow arrow indicates fragmented ZYP1 signals. Blue arrows indicate aggregated and/or enlarged ZYP1 foci. Scale bar = 10 μ m.

Parsed Citations

- Armstrong, S.J., Caryl, A.P., Jones, G.H., and Franklin, F.C. (2002). *Asy1*, a protein required for meiotic chromosome synapsis, localizes to axis-associated chromatin in *Arabidopsis* and *Brassica*. *J Cell Sci* 115, 3645-3655.
Google Scholar: [Author Only](#) [Title Only](#) [Author and Title](#)
- Bai, X., Peirson, B.N., Dong, F., Xue, C., and Makaroff, C.A. (1999). Isolation and Characterization of *SYN1*, a *RAD21*-like Gene Essential for Meiosis in *Arabidopsis*. *Plant Cell* 11, 417-430.
Google Scholar: [Author Only](#) [Title Only](#) [Author and Title](#)
- Barakate, A., Higgins, J.D., Vivera, S., Stephens, J., Perry, R.M., Ramsay, L., Colas, I., Oakey, H., Waugh, R., Franklin, F.C., Armstrong, S.J., and Halpin, C. (2014). The synaptonemal complex protein *ZYP1* is required for imposition of meiotic crossovers in barley. *Plant Cell* 26, 729-740.
Google Scholar: [Author Only](#) [Title Only](#) [Author and Title](#)
- Berchowitz, L.E., Francis, K.E., Bey, A.L., and Copenhaver, G.P. (2007). The role of *AtMUS81* in interference-insensitive crossovers in *A. thaliana*. *Plos Genetics* 3, e132.
Google Scholar: [Author Only](#) [Title Only](#) [Author and Title](#)
- Bergerat, A., de Massy, B., Gabelle, D., Varoutas, P.-C., Nicolas, A., and Forterre, P. (1997). An atypical topoisomerase II from archaea with implications for meiotic recombination. *Nature* 386, 414-417.
Google Scholar: [Author Only](#) [Title Only](#) [Author and Title](#)
- Bhatt, A.M., Canales, C., and Dickinson, H.G. (2001). Plant meiosis: the means to 1N. *Trends in Plant Science* 6, 114-121.
Google Scholar: [Author Only](#) [Title Only](#) [Author and Title](#)
- Bomblies, K., Higgins, J.D., and Yant, L. (2015). Meiosis evolves: adaptation to external and internal environments. *New Phytologist* 208, 306-323.
Google Scholar: [Author Only](#) [Title Only](#) [Author and Title](#)
- Bomblies, K., Jones, G., Franklin, C., Zickler, D., and Kleckner, N. (2016). The challenge of evolving stable polyploidy: could an increase in "crossover interference distance" play a central role? *Chromosoma* 125, 287-300.
Google Scholar: [Author Only](#) [Title Only](#) [Author and Title](#)
- Braz, G.T., Yu, F., Zhao, H., Deng, Z., Birchler, J.A., and Jiang, J. (2021). Preferential meiotic chromosome pairing among homologous chromosomes with cryptic sequence variation in tetraploid maize. *New Phytologist* 229, 3294-3302.
Google Scholar: [Author Only](#) [Title Only](#) [Author and Title](#)
- Bretagnolle, F., and Thompson, J.D. (1995). Gametes with the somatic chromosome number: mechanisms of their formation and role in the evolution of autopolyploid plants. *New Phytologist* 129, 1-22.
Google Scholar: [Author Only](#) [Title Only](#) [Author and Title](#)
- Cai, X., Dong, F., Edlmann, R.E., and Makaroff, C.A. (2003). The *Arabidopsis* *SYN1* cohesin protein is required for sister chromatid arm cohesion and homologous chromosome pairing. *J Cell Sci* 116, 2999-3007.
Google Scholar: [Author Only](#) [Title Only](#) [Author and Title](#)
- Capilla-Pérez, L., Durand, S., Hurel, A., Lian, Q., Chambon, A., Tauchy, C., Solier, V., Grelon, M., and Mercier, R. (2021). The synaptonemal complex imposes crossover interference and heterochiasmy in *Arabidopsis*. *Proc Natl Acad Sci U S A* 118, e2023613118.
Google Scholar: [Author Only](#) [Title Only](#) [Author and Title](#)
- Carballo, J.A., Panizza, S., Serrentino, M.E., Johnson, A.L., Geymonat, M., Borde, V., Klein, F., and Cha, R.S. (2013). Budding yeast *ATM/ATR* control meiotic double-strand break (DSB) levels by down-regulating *Rec114*, an essential component of the DSB-machinery. *Plos Genetics* 9, e1003545.
Google Scholar: [Author Only](#) [Title Only](#) [Author and Title](#)
- Chambon, A., West, A., Vezon, D., Horlow, C., De Muyt, A., Chelysheva, L., Ronceret, A., Darbyshire, A., Osman, K., Heckmann, S., Franklin, F.C.H., and Grelon, M. (2018). Identification of *ASYNAPTIC4*, a component of the meiotic chromosome axis. *Plant Physiology* 178, 233-246.
Google Scholar: [Author Only](#) [Title Only](#) [Author and Title](#)
- Chelysheva, L., Grandont, L., Vrielynck, N., Guin, S.I., Mercier, R., and Grelon, M. (2010). An easy protocol for studying chromatin and recombination protein dynamics during *Arabidopsis thaliana* meiosis: immunodetection of cohesins, histones and *MLH1*. *Cytogenetic and Genome Research* 129, 143-153.
Google Scholar: [Author Only](#) [Title Only](#) [Author and Title](#)
- Chelysheva, L., Diallo, S., Vezon, D., Gendrot, G., Vrielynck, N., Belcram, K., Rocques, N., Márquez-Lema, A., Bhatt, A.M., Horlow, C., Mercier, R., Mézard, C., and Grelon, M. (2005). *AtREC8* and *AtSCC3* are essential to the monopolar orientation of the kinetochores during meiosis. *Journal of Cell Science* 118, 4621-4632.
Google Scholar: [Author Only](#) [Title Only](#) [Author and Title](#)
- Cloud, V., Chan, Y.L., Grubb, J., Budke, B., and Bishop, D.K. (2012). *Rad51* is an accessory factor for *Dmc1*-mediated joint molecule formation during meiosis. *Science* 337, 1222-1225.

Google Scholar: [Author Only](#) [Title Only](#) [Author and Title](#)

Comai, L. (2005). The advantages and disadvantages of being polyploid. *Nat Rev Genet* 6, 836-846.

Google Scholar: [Author Only](#) [Title Only](#) [Author and Title](#)

Da Ines, O., Degroote, F., Goubely, C., Arniard, S., Gallego, M.E., and White, C.I. (2013). Meiotic recombination in *Arabidopsis* is catalysed by DMC1, with RAD51 playing a supporting role. *Plos Genetics* 9, e1003787.

Google Scholar: [Author Only](#) [Title Only](#) [Author and Title](#)

Da Ines, O., Michard, R., Fayos, I., Bastianelli, G., Nicolas, A., Guiderdoni, E., White, C., and Sourdille, P. (2020). Bread wheat TaSPO11-1 exhibits evolutionarily conserved function in meiotic recombination across distant plant species. *Plant Journal* 103, 2052-2068.

Google Scholar: [Author Only](#) [Title Only](#) [Author and Title](#)

De Muyt, A., Vezon, D., Gendrot, G., Gallois, J.-L., Stevens, R., and Grelon, M. (2007). AtPRD1 is required for meiotic double strand break formation in *Arabidopsis thaliana*. *EMBO Journal* 26, 4126-4137.

Google Scholar: [Author Only](#) [Title Only](#) [Author and Title](#)

De Storme, N., and Geelen, D. (2011). The *Arabidopsis* mutant jason produces unreduced first division restitution male gametes through a parallel/fused spindle mechanism in meiosis II. *Plant Physiology* 155, 1403-1415.

Google Scholar: [Author Only](#) [Title Only](#) [Author and Title](#)

De Storme, N., and Geelen, D. (2013). Cytokinesis in plant male meiosis. *Plant Signaling & Behavior* 8, e23394.

Google Scholar: [Author Only](#) [Title Only](#) [Author and Title](#)

De Storme, N., and Geelen, D. (2014). The impact of environmental stress on male reproductive development in plants: biological processes and molecular mechanisms. *Plant Cell and Environment* 37, 1-18.

Google Scholar: [Author Only](#) [Title Only](#) [Author and Title](#)

De Storme, N., and Geelen, D. (2020). High temperatures alter cross-over distribution and induce male meiotic restitution in *Arabidopsis thaliana*. *Communications Biology* 3, 187.

Google Scholar: [Author Only](#) [Title Only](#) [Author and Title](#)

De Storme, N., Copenhaver, G.P., and Geelen, D. (2012). Production of diploid male gametes in *Arabidopsis* by cold-induced destabilization of postmeiotic radial microtubule arrays. *Plant Physiology* 160, 1808-1826.

Google Scholar: [Author Only](#) [Title Only](#) [Author and Title](#)

Del Pozo, J.C., and Ramirez-Parra, E. (2015). Whole genome duplications in plants: an overview from *Arabidopsis*. *Journal of Experimental Botany* 66, 6991-7003.

Google Scholar: [Author Only](#) [Title Only](#) [Author and Title](#)

Draeger, T., and Moore, G. (2017). Short periods of high temperature during meiosis prevent normal meiotic progression and reduce grain number in hexaploid wheat (*Triticum aestivum* L.). *Theoretical and Applied Genetics* 130, 1785-1800.

Google Scholar: [Author Only](#) [Title Only](#) [Author and Title](#)

Dubcovsky, J., and Dvorak, J. (2007). Genome plasticity a key factor in the success of polyploid wheat under domestication. *Science* 316, 1862-1866.

Google Scholar: [Author Only](#) [Title Only](#) [Author and Title](#)

Ferdous, M., Higgins, J.D., Osman, K., Lambing, C., Roitinger, E., Mechtler, K., Armstrong, S.J., Perry, R., Pradillo, M., Cuñado, N., and Franklin, F.C.H. (2012). Inter-homolog crossing-over and synapsis in *Arabidopsis* meiosis are dependent on the chromosome axis protein AtASY3. *Plos Genetics* 8, e1002507-e1002507.

Google Scholar: [Author Only](#) [Title Only](#) [Author and Title](#)

Folk, R.A., Siniscalchi, C.M., and Soltis, D.E. (2020). Angiosperms at the edge: extremity, diversity, and phylogeny. *Plant Cell and Environment* 43, 2871-2893.

Google Scholar: [Author Only](#) [Title Only](#) [Author and Title](#)

France, M.G., Enderle, J., Röhrig, S., Puchta, H., Franklin, F.C.H., and Higgins, J.D. (2021). ZYP1 is required for obligate cross-over formation and cross-over interference in *Arabidopsis*. *Proc Natl Acad Sci U S A* 118.

Google Scholar: [Author Only](#) [Title Only](#) [Author and Title](#)

Garcia, V., Gray, S., Allison, R.M., Cooper, T.J., and Neale, M.J. (2015). Tel1/ATM-mediated interference suppresses clustered meiotic double-strand-break formation. *Nature* 520, 114-118.

Google Scholar: [Author Only](#) [Title Only](#) [Author and Title](#)

Grandont, L., Cuñado, N., Coriton, O., Huteau, V., Eber, F., Chèvre, A.M., Grelon, M., Chelysheva, L., and Jenczewski, E. (2014). Homeologous chromosome sorting and progression of meiotic recombination in *Brassica napus*: ploidy does matter! *Plant Cell* 26, 1448-1463.

Google Scholar: [Author Only](#) [Title Only](#) [Author and Title](#)

Grelon, M., Vezon, D., Gendrot, G., and Pelletier, G. (2001). AtSPO11-1 is necessary for efficient meiotic recombination in plants. *Embo j* 20, 589-600.

Google Scholar: [Author Only](#) [Title Only](#) [Author and Title](#)

- Hartung, F., Wurz-Wildersinn, R., Fuchs, J., Schubert, I., Suer, S., and Puchta, H. (2007). The catalytically active tyrosine residues of both SPO11-1 and SPO11-2 are required for meiotic double-strand break induction in *Arabidopsis*. *Plant Cell* 19, 3090-3099.
Google Scholar: [Author Only](#) [Title Only](#) [Author and Title](#)
- Henry, I.M., Dilkes, B.P., Tyagi, A., Gao, J., Christensen, B., and Comai, L. (2014). The BOY NAMED SUE quantitative trait locus confers increased meiotic stability to an adapted natural allopolyploid of *Arabidopsis*. *Plant Cell* 26, 181-194.
Google Scholar: [Author Only](#) [Title Only](#) [Author and Title](#)
- Higgins, J.D., Armstrong, S.J., Franklin, F.C.H., and Jones, G.H. (2004). The *Arabidopsis* MutS homolog AtMSH4 functions at an early step in recombination: evidence for two classes of recombination in *Arabidopsis*. *Genes & Development* 18, 2557-2570.
Google Scholar: [Author Only](#) [Title Only](#) [Author and Title](#)
- Higgins, J.D., Sanchez-Moran, E., Armstrong, S.J., Jones, G.H., and Franklin, F.C. (2005). The *Arabidopsis* synaptonemal complex protein ZYP1 is required for chromosome synapsis and normal fidelity of crossing over. *Genes & Development* 19, 2488-2500.
Google Scholar: [Author Only](#) [Title Only](#) [Author and Title](#)
- Hollingsworth, N.M., and Brill, S.J. (2004). The Mus81 solution to resolution: generating meiotic crossovers without Holliday junctions. *Genes & Development* 18, 117-125.
Google Scholar: [Author Only](#) [Title Only](#) [Author and Title](#)
- Jackson, S., and Chen, Z.J. (2010). Genomic and expression plasticity of polyploidy. *Current Opinion in Plant Biology* 13, 153-159.
Google Scholar: [Author Only](#) [Title Only](#) [Author and Title](#)
- Joyce, E.F., Pedersen, M., Tiong, S., White-Brown, S.K., Paul, A., Campbell, S.D., and McKim, K.S. (2011). *Drosophila* ATM and ATR have distinct activities in the regulation of meiotic DNA damage and repair. *Journal of Cell Biology* 195, 359-367.
Google Scholar: [Author Only](#) [Title Only](#) [Author and Title](#)
- Kim, J., and Choi, K. (2019). Signaling-mediated meiotic recombination in plants. *Current Opinion in Plant Biology* 51, 44-50.
Google Scholar: [Author Only](#) [Title Only](#) [Author and Title](#)
- Klimyuk, V.I., and Jones, J.D.G. (1997). AtDMC1, the *Arabidopsis* homologue of the yeast DMC1 gene: characterization, transposon-induced allelic variation and meiosis-associated expression. *Plant Journal* 11, 1-14.
Google Scholar: [Author Only](#) [Title Only](#) [Author and Title](#)
- Kobayashi, W., Liu, E., Ishii, H., Matsunaga, S., Schlogelhofer, P., and Kurumizaka, H. (2019). Homologous pairing activities of *Arabidopsis thaliana* RAD51 and DMC1. *J Biochem* 165, 289-295.
Google Scholar: [Author Only](#) [Title Only](#) [Author and Title](#)
- Kurzbauer, M.-T., Janisiw, M.P., Paulin, L.F., Prusén Mota, I., Tomanov, K., Krsicka, O., Haeseler, A.v., Schubert, V., and Schlogelhofer, P. (2021). ATM controls meiotic DNA double-strand break formation and recombination and affects synaptonemal complex organization in plants. *The Plant Cell*.
Google Scholar: [Author Only](#) [Title Only](#) [Author and Title](#)
- Kurzbauer, M.T., Uanschou, C., Chen, D., and Schlogelhofer, P. (2012). The recombinases DMC1 and RAD51 are functionally and spatially separated during meiosis in *Arabidopsis*. *Plant Cell* 24, 2058-2070.
Google Scholar: [Author Only](#) [Title Only](#) [Author and Title](#)
- Lambing, C., Kuo, P.C., Tock, A.J., Topp, S.D., and Henderson, I.R. (2020a). ASY1 acts as a dosage-dependent antagonist of telomere-led recombination and mediates crossover interference in *Arabidopsis*. *Proc Natl Acad Sci U S A* 117, 13647-13658.
Google Scholar: [Author Only](#) [Title Only](#) [Author and Title](#)
- Lambing, C., Tock, A.J., Topp, S.D., Choi, K., Kuo, P.C., Zhao, X., Osman, K., Higgins, J.D., Franklin, F.C.H., and Henderson, I.R. (2020b). Interacting genomic landscapes of REC8-cohesin, chromatin, and meiotic recombination in *Arabidopsis*. *Plant Cell* 32, 1218-1239.
Google Scholar: [Author Only](#) [Title Only](#) [Author and Title](#)
- Lan, W.-H., Lin, S.-Y., Kao, C.-Y., Chang, W.-H., Yeh, H.-Y., Chang, H.-Y., Chi, P., and Li, H.-W. (2020). Rad51 facilitates filament assembly of meiosis-specific Dmc1 recombinase. *Proc Natl Acad Sci U S A* 117, 11257-11264.
Google Scholar: [Author Only](#) [Title Only](#) [Author and Title](#)
- Lange, J., Pan, J., Cole, F., Thelen, M.P., Jasin, M., and Keeney, S. (2011). ATM controls meiotic double-strand-break formation. *Nature* 479, 237-240.
Google Scholar: [Author Only](#) [Title Only](#) [Author and Title](#)
- Lei, X., Ning, Y., Eid Elesawi, I., Yang, K., Chen, C., Wang, C., and Liu, B. (2020). Heat stress interferes with chromosome segregation and cytokinesis during male meiosis in *Arabidopsis thaliana*. *Plant Signaling & Behavior* 15, 1746985.
Google Scholar: [Author Only](#) [Title Only](#) [Author and Title](#)
- Leitch, A.R., and Leitch, I.J. (2008). Genomic plasticity and the diversity of polyploid plants. *Science* 320, 481-483.
Google Scholar: [Author Only](#) [Title Only](#) [Author and Title](#)
- Li, W., and Yanowitz, J.L. (2019). ATM and ATR influence meiotic crossover formation through antagonistic and overlapping functions in *Caenorhabditis elegans*. *Genetics* 212, 431-443.
Google Scholar: [Author Only](#) [Title Only](#) [Author and Title](#)

- Li, W., Chen, C., Markmann-Mulisch, U., Timofejeva, L., Schmelzer, E., Ma, H., and Reiss, B. (2004). The Arabidopsis *AtRAD51* gene is dispensable for vegetative development but required for meiosis. *Proc Natl Acad Sci U S A* 101, 10596-10601.
Google Scholar: [Author Only](#) [Title Only](#) [Author and Title](#)
- Liu, B., De Storme, N., and Geelen, D. (2017). Cold interferes with male meiotic cytokinesis in *Arabidopsis thaliana* independently of the *AHK2/3-AHP2/3/5* cytokinin signaling module. *Cell Biology International* 41, 879-889.
Google Scholar: [Author Only](#) [Title Only](#) [Author and Title](#)
- Liu, B., De Storme, N., and Geelen, D. (2018). Cold-induced male meiotic restitution in *Arabidopsis thaliana* is not mediated by *GA-DELLA* signaling. *Frontiers in Plant Science* 9, 91.
Google Scholar: [Author Only](#) [Title Only](#) [Author and Title](#)
- Liu, B., Mo, W.J., Zhang, D., De Storme, N., and Geelen, D. (2019). Cold influences male reproductive development in plants: a hazard to fertility, but a window for evolution. *Plant Cell Physiology* 60, 7-18.
Google Scholar: [Author Only](#) [Title Only](#) [Author and Title](#)
- Lloyd, A., and Bomblies, K. (2016). Meiosis in autopolyploid and allopolyploid *Arabidopsis*. *Current Opinion in Plant Biology* 30, 116-122.
Google Scholar: [Author Only](#) [Title Only](#) [Author and Title](#)
- Lloyd, A., Morgan, C., H. Franklin, F.C., and Bomblies, K. (2018). Plasticity of Meiotic Recombination Rates in Response to Temperature in *Arabidopsis*. *Genetics* 208, 1409-1420.
Google Scholar: [Author Only](#) [Title Only](#) [Author and Title](#)
- Lohani, N., Singh, M.B., and Bhalla, P.L. (2019). High temperature susceptibility of sexual reproduction in crop plants. *Journal of Experimental Botany* 71, 555-568.
Google Scholar: [Author Only](#) [Title Only](#) [Author and Title](#)
- Loidl, J. (1989). Effects of elevated temperature on meiotic chromosome synapsis in *Allium ursinum*. *Chromosoma* 97, 449-458.
Google Scholar: [Author Only](#) [Title Only](#) [Author and Title](#)
- Lourkisti, R., Froelicher, Y., Herbet, S., Morillon, R., Tomi, F., Gibernau, M., Giannettini, J., Berti, L., and Santini, J. (2020). Triploid citrus genotypes have a better tolerance to natural chilling conditions of photosynthetic capacities and specific leaf volatile organic compounds. *Frontiers in Plant Science* 11.
Google Scholar: [Author Only](#) [Title Only](#) [Author and Title](#)
- Mai, Y., Li, H., Suo, Y., Fu, J., Sun, P., Han, W., Diao, S., and Li, F. (2019). High temperature treatment generates unreduced pollen in persimmon (*Diospyros kaki* Thunb.). *Scientia Horticulturae* 258, 108774.
Google Scholar: [Author Only](#) [Title Only](#) [Author and Title](#)
- Modliszewski, J.L., Wang, H., Albright, A.R., Lewis, S.M., Bennett, A.R., Huang, J., Ma, H., Wang, Y., and Copenhaver, G.P. (2018). Elevated temperature increases meiotic crossover frequency via the interfering (Type I) pathway in *Arabidopsis thaliana*. *Plos Genetics* 14, e1007384.
Google Scholar: [Author Only](#) [Title Only](#) [Author and Title](#)
- Mohibullah, N., and Keeney, S. (2017). Numerical and spatial patterning of yeast meiotic DNA breaks by Tel1. *Genome Research* 27, 278-288.
Google Scholar: [Author Only](#) [Title Only](#) [Author and Title](#)
- Morgan, C., Zhang, H., Henry, C.E., Franklin, F.C.H., and Bomblies, K. (2020). Derived alleles of two axis proteins affect meiotic traits in autotetraploid *Arabidopsis arenosa*. *Proc Natl Acad Sci U S A* 117, 8980-8988.
Google Scholar: [Author Only](#) [Title Only](#) [Author and Title](#)
- Morgan, C.H., Zhang, H., and Bomblies, K. (2017). Are the effects of elevated temperature on meiotic recombination and thermotolerance linked via the axis and synaptonemal complex? *Philos Trans R Soc Lond B Biol Sci* 372, 20160470.
Google Scholar: [Author Only](#) [Title Only](#) [Author and Title](#)
- Ning, Y., Liu, Q., Wang, C., Qin, E., Wu, Z., Wang, M., Yang, K., Elesawi, I.E., Chen, C., Liu, H., Qin, R., and Liu, B. (2020). Heat stress interferes with formation of double-strand breaks and homolog synapsis in *Arabidopsis thaliana*. *BioRxiv*, 2020.2010.2002.324269.
Google Scholar: [Author Only](#) [Title Only](#) [Author and Title](#)
- Ning, Y., Liu, Q., Wang, C., Qin, E., Wu, Z., Wang, M., Yang, K., Elesawi, I.E., Chen, C., Liu, H., Qin, R., and Liu, B. (2021). Heat stress interferes with formation of double-strand breaks and homolog synapsis. *Plant Physiology*.
Google Scholar: [Author Only](#) [Title Only](#) [Author and Title](#)
- Osman, K., Yang, J., Roitinger, E., Lambing, C., Heckmann, S., Howell, E., Cuacos, M., Imre, R., Durnberger, G., Mechtler, K., Armstrong, S., and Franklin, F.C.H. (2018). Affinity proteomics reveals extensive phosphorylation of the Brassica chromosome axis protein *ASY1* and a network of associated proteins at prophase I of meiosis. *Plant Journal* 93, 17-33.
Google Scholar: [Author Only](#) [Title Only](#) [Author and Title](#)
- Otto, S.P. (2007). The evolutionary consequences of polyploidy. *Cell* 131, 452-462.
Google Scholar: [Author Only](#) [Title Only](#) [Author and Title](#)
- Parisod, C., Holderegger, R., and Brochmann, C. (2010). Evolutionary consequences of autopolyploidy. *New Phytologist* 186, 5-17.
Google Scholar: [Author Only](#) [Title Only](#) [Author and Title](#)

- Paull, T.T. (2015). Mechanisms of ATM activation. *Annu Rev Biochem* 84, 711-738.
Google Scholar: [Author Only](#) [Title Only](#) [Author and Title](#)
- Pohl, T.J., and Nickoloff, J.A. (2008). Rad51-independent interchromosomal double-strand break repair by gene conversion requires Rad52 but not Rad55, Rad57, or Dmc1. *Molecular and cellular biology* 28, 897-906.
Google Scholar: [Author Only](#) [Title Only](#) [Author and Title](#)
- Ramsey, J., and Schemske, D.W. (1998). Pathways, mechanisms, and rates of polyploid formation in flowering plants. *Annual Review of Ecology and Systematics* 29, 467-501.
Google Scholar: [Author Only](#) [Title Only](#) [Author and Title](#)
- Ramsey, J., and Schemske, D.W. (2002). Neopolyploidy in flowering plants. *Annual Review of Ecology and Systematics* 33, 589-639.
Google Scholar: [Author Only](#) [Title Only](#) [Author and Title](#)
- Rao, S., Tian, Y., Xia, X., Li, Y., and Chen, J. (2020). Chromosome doubling mediates superior drought tolerance in *Lycium ruthenicum* via abscisic acid signaling. *Hortic Res* 7, 40.
Google Scholar: [Author Only](#) [Title Only](#) [Author and Title](#)
- Ren, R., Wang, H.F., Guo, C.C., Zhang, N., Zeng, L.P., Chen, Y.M., Ma, H., and Qi, J. (2018). Widespread whole genome duplications contribute to genome complexity and species diversity in angiosperms. *Molecular Plant* 11, 414-428.
Google Scholar: [Author Only](#) [Title Only](#) [Author and Title](#)
- Sanchez-Moran, E., Santos, J.L., Jones, G.H., and Franklin, F.C. (2007). ASY1 mediates AtDMC1-dependent interhomolog recombination during meiosis in *Arabidopsis*. *Genes & Development* 21, 2220-2233.
Google Scholar: [Author Only](#) [Title Only](#) [Author and Title](#)
- Santos, J.L., Alfaro, D., Sanchez-Moran, E., Armstrong, S.J., Franklin, F.C.H., and Jones, G.H. (2003). Partial diploidization of meiosis in autotetraploid *Arabidopsis thaliana*. *Genetics* 165, 1533-1540.
Google Scholar: [Author Only](#) [Title Only](#) [Author and Title](#)
- Seear, P.J., France, M.G., Gregory, C.L., Heavens, D., Schmickl, R., Yant, L., and Higgins, J.D. (2020). A novel allele of ASY3 is associated with greater meiotic stability in autotetraploid *Arabidopsis lyrata*. *Plos Genetics* 16, e1008900-e1008900.
Google Scholar: [Author Only](#) [Title Only](#) [Author and Title](#)
- Shahid, S. (2020). The rules of attachment: REC8 cohesin connects chromatin architecture and recombination machinery in meiosis. *Plant Cell* 32, 808-809.
Google Scholar: [Author Only](#) [Title Only](#) [Author and Title](#)
- Shi, W., Ji, J., Xue, Z., Zhang, F., Miao, Y., Yang, H., Tang, D., Du, G., Li, Y., Shen, Y., and Cheng, Z. (2021). PRD1, a homologous recombination initiation factor, is involved in spindle assembly in rice meiosis. *New Phytologist* 230, 585-600.
Google Scholar: [Author Only](#) [Title Only](#) [Author and Title](#)
- Singh, G., Da Ines, O., Gallego, M.E., and White, C.I. (2017). Analysis of the impact of the absence of RAD51 strand exchange activity in *Arabidopsis* meiosis. *Plos One* 12, e0183006.
Google Scholar: [Author Only](#) [Title Only](#) [Author and Title](#)
- Soltis, P.S., and Soltis, D.E. (2009). The role of hybridization in plant speciation. *Annual Review of Plant Biology* 60, 561-588.
Google Scholar: [Author Only](#) [Title Only](#) [Author and Title](#)
- Soltis, P.S., Marchant, D.B., Van de Peer, Y., and Soltis, D.E. (2015). Polyploidy and genome evolution in plants. *Current Opinion in Genetics & Development* 35, 119-125.
Google Scholar: [Author Only](#) [Title Only](#) [Author and Title](#)
- Stacey, N.J., Kuromori, T., Azumi, Y., Roberts, G., Breuer, C., Wada, T., Maxwell, A., Roberts, K., and Sugimoto-Shirasu, K. (2006). *Arabidopsis* SPO11-2 functions with SPO11-1 in meiotic recombination. *Plant Journal* 48, 206-216.
Google Scholar: [Author Only](#) [Title Only](#) [Author and Title](#)
- Stift, M., Berenos, C., Kuperus, P., and van Tienderen, P.H. (2008). Segregation models for disomic, tetrasomic and intermediate inheritance in tetraploids: a general procedure applied to rorippa (Yellow Cress) microsatellite data. *Genetics* 179, 2113-2123.
Google Scholar: [Author Only](#) [Title Only](#) [Author and Title](#)
- Su, H., Cheng, Z., Huang, J., Lin, J., Copenhaver, G.P., Ma, H., and Wang, Y. (2017). *Arabidopsis* RAD51, RAD51C and XRCC3 proteins form a complex and facilitate RAD51 localization on chromosomes for meiotic recombination. *Plos Genetics* 13, e1006827.
Google Scholar: [Author Only](#) [Title Only](#) [Author and Title](#)
- Sugimoto-Shirasu, K., Stacey, N.J., Corsar, J., Roberts, K., and McCann, M.C. (2002). DNA topoisomerase VI is essential for endoreduplication in *Arabidopsis*. *Curr Biol* 12, 1782-1786.
Google Scholar: [Author Only](#) [Title Only](#) [Author and Title](#)
- Svačina, R., Sourdille, P., Kopecký, D., and Bartoš, J. (2020). Chromosome pairing in polyploid grasses. *Frontiers in Plant Science* 11, 1056.
Google Scholar: [Author Only](#) [Title Only](#) [Author and Title](#)

- Tang, Z., Zhang, L., Yang, D., Zhao, C., and Zheng, Y. (2011). Cold stress contributes to aberrant cytokinesis during male meiosis I in a wheat thermosensitive genic male sterile line. *Plant Cell and Environment* 34, 389-405.
Google Scholar: [Author Only](#) [Title Only](#) [Author and Title](#)
- te Beest, M., Le Roux, J.J., Richardson, D.M., Brysting, A.K., Suda, J., Kubesová, M., and Pysek, P. (2012). The more the better? The role of polyploidy in facilitating plant invasions. *Ann Bot* 109, 19-45.
Google Scholar: [Author Only](#) [Title Only](#) [Author and Title](#)
- Uanschou, C., Siwiec, T., Pedrosa-Harand, A., Kerzendorfer, C., Sanchez-Moran, E., Novatchkova, M., Akimcheva, S., Woglar, A., Klein, F., and Schlögelhofer, P. (2007). A novel plant gene essential for meiosis is related to the human CtIP and the yeast COM1/SAE2 gene. *EMBO Journal* 26, 5061-5070.
Google Scholar: [Author Only](#) [Title Only](#) [Author and Title](#)
- Van de Peer, Y., Ashman, T.-L., Soltis, P.S., and Soltis, D.E. (2020). Polyploidy: an evolutionary and ecological force in stressful times. *Plant Cell* 33, 11-26.
Google Scholar: [Author Only](#) [Title Only](#) [Author and Title](#)
- Wang, J., Li, D., Shang, F., and Kang, X. (2017). High temperature-induced production of unreduced pollen and its cytological effects in *Populus*. *Scientific Reports* 7, 5281.
Google Scholar: [Author Only](#) [Title Only](#) [Author and Title](#)
- Wang, M., Wang, K., Tang, D., Wei, C., Li, M., Shen, Y., Chi, Z., Gu, M., and Cheng, Z. (2010). The central element protein ZEP1 of the synaptonemal complex regulates the number of crossovers during meiosis in rice. *Plant Cell* 22, 417-430.
Google Scholar: [Author Only](#) [Title Only](#) [Author and Title](#)
- Wang, Y., and Copenhaver, G.P. (2018). Meiotic recombination: mixing it up in plants. *Annual Review of Plant Biology* 69, 577-609.
Google Scholar: [Author Only](#) [Title Only](#) [Author and Title](#)
- Wang, Y., Cheng, Z., Lu, P., Timofejeva, L., and Ma, H. (2014). Molecular cell biology of male meiotic chromosomes and isolation of male meiocytes in *Arabidopsis thaliana*. *Methods Mol Biol* 1110, 217-230.
Google Scholar: [Author Only](#) [Title Only](#) [Author and Title](#)
- Wu, S., Han, B., and Jiao, Y. (2020). Genetic contribution of paleopolyploidy to adaptive evolution in angiosperms. *Molecular Plant* 13, 59-71.
Google Scholar: [Author Only](#) [Title Only](#) [Author and Title](#)
- Xue, M., Wang, J., Jiang, L., Wang, M., Wolfe, S., Pawlowski, W.P., Wang, Y., and He, Y. (2018). The number of meiotic double-strand breaks influences crossover distribution in *Arabidopsis*. *Plant Cell* 30, 2628-2638.
Google Scholar: [Author Only](#) [Title Only](#) [Author and Title](#)
- Xue, Z., Liu, C., Shi, W., Miao, Y., Shen, Y., Tang, D., Li, Y., You, A., Xu, Y., Chong, K., and Cheng, Z. (2019). OsMTOPIB is required for meiotic bipolar spindle assembly. *Proc Natl Acad Sci U S A* 116, 15967-15972.
Google Scholar: [Author Only](#) [Title Only](#) [Author and Title](#)
- Yant, L., Hollister, J.D., Wright, K.M., Arnold, B.J., Higgins, J.D., Franklin, F.C.H., and Bomblies, K. (2013). Meiotic adaptation to genome duplication in *Arabidopsis arenosa*. *Current Biology* 23, 2151-2156.
Google Scholar: [Author Only](#) [Title Only](#) [Author and Title](#)
- Yao, Y., Li, X., Chen, W., Liu, H., Mi, L., Ren, D., Mo, A., and Lu, P. (2020). ATM Promotes RAD51-Mediated Meiotic DSB Repair by Inter-Sister-Chromatid Recombination in *Arabidopsis*. *Frontiers in Plant Science* 11, 839.
Google Scholar: [Author Only](#) [Title Only](#) [Author and Title](#)
- Yin, Y., Cheong, H., Friedrichsen, D., Zhao, Y., Hu, J., Mora-Garcia, S., and Chory, J. (2002). A crucial role for the putative *Arabidopsis* topoisomerase VI in plant growth and development. *Proc Natl Acad Sci U S A* 99, 10191-10196.
Google Scholar: [Author Only](#) [Title Only](#) [Author and Title](#)
- Zamariola, L., Tiang, C.L., De Storme, N., Pawlowski, W., and Geelen, D. (2014). Chromosome segregation in plant meiosis. *Frontiers in Plant Science* 5, 279.
Google Scholar: [Author Only](#) [Title Only](#) [Author and Title](#)
- Zhang, L., Kim, K.P., Kleckner, N.E., and Storlazzi, A. (2011). Meiotic double-strand breaks occur once per pair of (sister) chromatids and, via Mec1/ATR and Tel1/ATM, once per quartet of chromatids. *Proceedings of the National Academy of Sciences of the United States of America* 108, 20036-20041.
Google Scholar: [Author Only](#) [Title Only](#) [Author and Title](#)
- Zickler, D., and Kleckner, N. (1999). Meiotic chromosomes: integrating structure and function. *Annu Rev Genet* 33, 603-754.
Google Scholar: [Author Only](#) [Title Only](#) [Author and Title](#)